Arabian Journal of Chemistry (2022) **15**, 103898

King Saud University

**Arabian Journal of Chemistry**

www.ksu.edu.sa
www.sciencedirect.com

ORIGINAL ARTICLE

# Molecular modeling and docking studies of new antimicrobial antipyrine-thiazole hybrids

**Sraa Abu-Melha**

*Department of Chemistry, Faculty of Science, King Khalid University, Abha 62529, Saudi Arabia*

Received 1 October 2021; accepted 3 April 2022
Available online 9 April 2022

**KEYWORDS**

Antipyrine;
Thiosemicarbazone;
Ethyl bromoacetate;
Antibacterial;
Molecular docking

**Abstract** A series of new antipyrine incorporated thiazole derivatives having phenoxyacetamide moiety as a link bridge was synthesized. The synthetic strategy involves condensation of the precursor *N*-(4-antipyrinyl)-2-(4-formylphenoxy)acetamide with thiosemicarbazide followed by heterocyclization of the produced thiosemicarbazone with various α-halogenated carbonyl compounds (namely; 4-chlorophenacyl bromide, ethyl bromoacetate, 3-chloroacetylacetone and ethyl 4-chloroacetoacetate). Moreover, the quantum chemical calculations at DFT/B3LYP level were used to determine the HOMO-LUMO energies and Fukui's indices toward nucleophilic, electrophilic and radical attacks. The investigated compounds were arranged due to HOMO-LUMO energy gap as following **6** < **5** < **7** < **3** < **2** < **4** < **8**. The synthesized antipyrinyl-thiazole hybrids were screened to evaluate their antibacterial and antifungal efficacies. Using Chloramphenicol as reference material, the synthesized antipyrinyl-thiazole hybrids were revealed a remarkable activity against *S. aureus* than *B. subtilis*, as example for Gram's positive strains. The antipyrine-thiazole compounds **3**, **4**, **6** and **8** exhibited significant MIC values. However, the antipyrine-thiazole hybride **4** displayed reputable activities against Gram's negative strains *S. typhimurium* and *E. coli*, respectively, in comparison with Cephalothin. Likewise, the compounds **7** and **8** were demonstrated respectable antifungal efficacy toward *C. albicans* in contrast to cycloheximide grade. The theoretical molecular docking studies were applied to simulate reactivity of the synthesized antipyrine-thiazole hybrids against contrasting binding sites for both of *Staphylococcus aureus* "Homo sapiens" (pdb: 3HUN) protein and *E.coli* "Homo sapiens" (PDB: 2EXB) protein. The theoretical and practical antibacterial and antifungal activities result in this work designated a proper agreement.

© 2022 The Author(s). Published by Elsevier B.V. on behalf of King Saud University. This is an open access article under the CC BY license (http://creativecommons.org/licenses/by/4.0/).

## 1. Introduction

Pyrazolone derivatives are important heterocycles, which exhibit pronounced pharmacological properties. Especially, antipyrine (1,2-dihy dro-1,5-dimethyl-2-phenyl-3H-pyrazol-3-one) is a biological versatile structure due to the presence of tribioactive centers like methyl, N and O groups, which generates interest in the studies of antipyrine

E-mail address: sabomlha@kku.edu.sa
Peer review under responsibility of King Saud University.

Production and hosting by Elsevier

https://doi.org/10.1016/j.arabjc.2022.103898
1878-5352 © 2022 The Author(s). Published by Elsevier B.V. on behalf of King Saud University.
This is an open access article under the CC BY license (http://creativecommons.org/licenses/by/4.0/).

derivatives. 4-Aminoantipyrine and its derivatives exhibit a fascinating array of pharmacological activity imputed to their ability to have non covalent interactions with various active site in organism (Jaiswal et al., 2014). Examples of antipyrine derivatives commercialized as antibacterial (Singh et al., 2020), non-steroidal anti-inflammatory (Mahle et al., 2010, Remes et al., 2012) and anti-cancer (Ibáñez et al., 2005) drugs are provided in Fig. 1. The therapeutic effect of antipyrine is due to the ability to inhibit cyclooxygenase isoforms (COX-1 and COX-2) and prostaglandin $H_2$ synthase enzymes, thus preventing the development of the main mediators of inflammation and pain (El Sayed et al., 2018).

On the other hand, thiazole is important heterocyclic compound that found in many potent biologically active molecules such as Sulfathiazole (antimicrobial drug), Ritonavir (antiretroviral drug), Abafungin (antifungal drug) with trade name Abasol cream and Bleomycine and Tiazofurin (antineoplastic drug) (Siddiqui et al., 2009). Thiazole and its derivatives had effective applications in medical area. They are used for the treatment of hypertension (Bagheri et al., 2004), inflammation (Deb et al., 2014), schizophrenia (Jaen et al., 1990), bacterial infections (Biernasiuk et al., 2019), and HIV infections (Rauf et al., 2019). They were also utilized as fibrinogen receptor antagonists with antithrombotic activity (Badorc et al., 1997) and as inhibitors of bacterial DNA gyrase B (Rudolph et al., 2001). Many thiazole scaffolds have been found to possess significant antitumor activity, such as the marketed anti-cancer drugs Dasatinib (Lombardo et al., 2004) and Dabrafenib (Dhillon, 2016) with potent antiproliferative activity (Fig. 1).

In view of the above-mentioned findings, we decided to develop some novel structure hybrids incorporating the antipyrine with thiazole ring systems through acetamide linkage. Such combination was suggested in an attempt to explore the influence of such hybridization and structure variation on the expected antibacterial activity, hoping to add some biological significance to the target compounds. Thus, our synthetic strategy for antipyrine-thiazole hybrids was achieved based on the synthesis of *N*-(4-antipyrinyl)-2-(4-formylphenoxy)acetamide (**2**), which was utilized through its 4-formylphenoxy moiety as a precursor for the building of thiazole ring. The evaluation of antimicrobial properties of the constructed thiazole-pyridine hybrids was carried out towards diverse pathogenic strains, such as gram-positive bacteria (*Staphylococcus aureus* and *Bacillus subtilis*), gram-negative bacteria (*Salmonella typhimurium and Escherichia coli*), and fungi (*Candida albicans* and *Aspergillus fumigatus*).

## 2. Experimental

### 2.1. Synthesis of antipyrine-thiazole hybrids 4, 5, 6, 7 and 8

Melting points were determined on Gallenkamp electric device and are uncorrected. IR spectra were registered on Thermo Scientific Nicolet iS10 FTIR spectrometer. $^1$H NMR (500 MHz) and $^{13}$C NMR (125 MHz) spectra were measured on JOEL's instrument (DMSO $d_6$ is used as solvent). The mass spectra were determined on Quadrupole GC–MS (DSQII) mass spectrometer at 70 eV.

#### 2.1.1. Synthesis of N-(4-antipyrinyl)-2-(4-formylphenoxy) acetamide (2)

In 100 mL conical flask, a suspension of *N*-(4-antipyrinyl)-2-chloroacetamide (**1**) (1.70 g, 0.01 mol), 4-hydroxybenzaldehyde (1.22 g, 0.01 mol) and anhydrous $K_2CO_3$ (1.38 g, 0.01 mol) in 25 mL DMSO was stirred for 8 h. The mixture was poured onto ice-cold water (75–80 mL) and kept in refrigerator for 6 h. The solid that produced was filtered and recrystallized from ethanol to produce the corresponding benzaldehyde derivative **2**.

Yield = 78%, m.p. = 202–203 °C. IR (KBr) $\bar{\nu}$/cm$^{-1}$: 3196 (N-H), 1682 (CH = O), 1664 (N-C = O). $^1$H NMR (δ/ppm): 2.10 (s, 3H, $CH_3$), 3.04 (s, 3H, $CH_3$), 4.82 (s, 2H, $CH_2$), 7.17 (d, $J$ = 8.50 Hz, 2H, Ar-H), 7.33–7.49 (m, 5H, Ar-H), 7.89 (d, $J$ = 8.50 Hz, 2H, Ar-H), 9.40 (s, 1H, NH), 9.87 (s, 1H, CH = O). $^{13}$C NMR (δ/ppm): 12.62, 35.56, 67.13, 107.94, 115.19 (2C), 123.66 (2C), 124.09, 129.18 (2C), 130.46, 132.19 (2C), 133.87, 135.67, 160.81, 164.09, 167.54, 191.28. MS $m/z$ (%): 365 ($M^+$, 48.69). Anal. Calcd. for $C_{20}H_{19}N_3O_4$

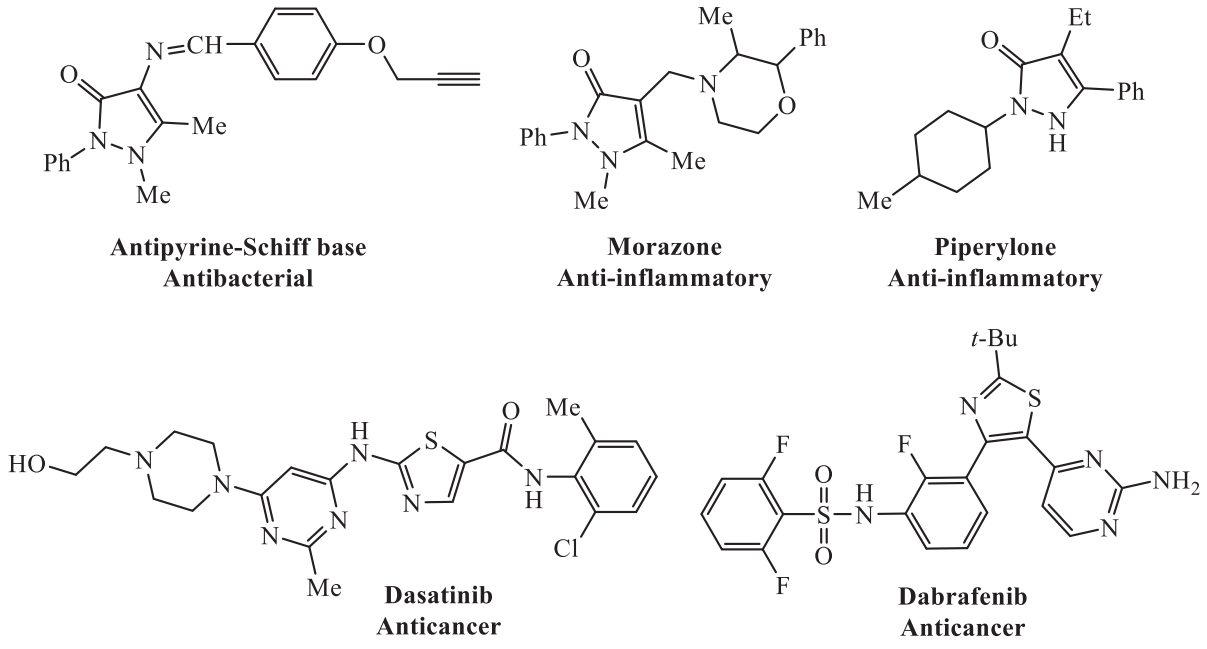


**Fig. 1** Selected biologically active antipyrine and thiazole structures.

(365.14): C, 65.74; H, 5.24; N, 11.50%. Found: C, 65.88; H, 5.20; N, 11.42%.

*2.1.2. Synthesis of N-(4-antipyrinyl)-2-(4-((2-carbamothioylhydrazono)methyl)phenoxy)-acetamide (**3**):*

A 100 mL RBF was charged with *N*-(4-antipyrinyl)-2-(4-formylphenoxy)acetamide (**2**) (1.82 g, 5 mmol). Then, thiosemicarbazide (0.46 g, 5 mmol), 50 mL ethanol and 1 mL acetic acid were added into the flask. The reaction mixture was refluxed for 4 h and then allowed to cool. The solid that formed was collected and recrystallized from EtOH/DMF mixture (8:1) to afford the thiosemicarbazone compound **3**.

Yield 71%, m.p. = 182–183 °C. IR (KBr): 3361, 3245, 3173 ($NH_2$ and NH), 1683 $cm^{-1}$ (C = O). $^1H$ NMR (δ/ppm): 2.14 (s, 3H, $CH_3$), 3.12 (s, 3H, $CH_3$), 4.76 (s, 2H, $CH_2$), 7.12 (d, $J$ = 8.50 Hz, 2H, Ar-H), 7.30–7.52 (m, 5H, Ar-H), 7.85 (d, $J$ = 8.50 Hz, 2H, Ar-H), 8.22 (s, 1H, $NH_a$), 8.34 (s, 1H, CH = N), 8.61 (s, 1H, $NH_b$), 10.32 (s, 1H, NH), 10.88 ppm (s, 1H, NH). $^{13}C$ NMR (δ/ppm): 12.58, 35.47, 67.16, 108.02, 114.91 (2C), 123.72 (2C), 124.31, 126.44, 129.15 (2C), 129.87 (2C), 134.11, 136.50, 146.30, 160.07, 160.85, 167.78, 179.05. MS $m/z$ (%): 438 ($M^+$, 44.52). Analysis for $C_{21}H_{22}N_6O_3S$ (438.15): Calcd: C, 57.52; H, 5.06; N, 19.17%. Found: C, 57.41; H, 5.11; N, 19.10%.

*2.1.3. Synthesis of N-(4-antipyrinyl)-2-(4-((2-(4-(4-chlorophenyl)thiazol-2-yl)hydrazono)methyl)phenoxy) acetamide (**4**):*

In 100 mL round-bottom flask, the thiosemicarbazone derivative **3** (0.87 g, 2 mmol) was dissolved in 40 mL ethanol, followed by subsequent addition of 4-chlorophenacyl bromide (0.46 g, 2 mmol) and triethylamine (0.2 mL). The reaction components were refluxed for 2 h and then allowed to cool at 20–25 °C. The solid that formed was collected and dried to furnish the corresponding antipyrine-thiazole hybrid **4**.

Yield 62%, m.p. = 264–265 °C. IR (KBr): 3234, 3188 (N-H), 1678 $cm^{-1}$ (C = O). $^1H$ NMR (δ/ppm): 2.21 (s, 3H, $CH_3$), 3.17 (s, 3H, $CH_3$), 4.68 (s, 2H, $CH_2$), 7.08 (d, $J$ = 8.00 Hz, 2H, Ar-H), 7.20 (s, 1H, thiazole-H5), 7.32–7.64 (m, 9H, Ar-H), 7.82 (d, $J$ = 8.00 Hz, 2H, Ar-H), 8.08 (s, 1H, CH = N), 10.36 (s, 1H, NH), 11.74 ppm (s, 1H, NH). $^{13}C$ NMR (δ/ppm): 12.46, 35.40, 67.20, 106.90, 108.14, 114.88 (2C), 123.75 (2C), 124.33, 126.50, 128.73 (2C), 129.11 (2C), 129.36 (2C), 129.94 (2C), 132.45, 133.79, 134.15, 136.58, 145.86, 148.06, 159.68, 160.89, 167.74, 170.82. MS $m/z$ (%): 574 ($M^+$ + 2, 8.26), 572 ($M^+$, 31.40). Analysis for $C_{29}H_{25}ClN_6O_3S$ (572.14): Calcd: C, 60.78; H, 4.40; N, 14.67%. Found: C, 60.96; H, 4.47; N, 14.54%.

*2.1.4. Synthesis of N-(4-antipyrinyl)-2-(4-((2-(4-oxo-4,5-dihydrothiazol-2-yl)hydrazono)-methyl)phenoxy)acetamide (**5**):*

To a suspension of thiosemicarbazone compound **3** (0.87 g, 2 mmol) in 40 mL ethanol, ethyl bromoacetate (0.34 mL, 2 mmol) and fused sodium acetate (0.5 g) were added. The reaction components were was heated under reflux for 4 h and then left to cool at 20–25 °C. The mixture was diluted with 40 mL cold water, the solid that obtained was collected and subjected to recrystallization from EtOH-DMF mixture (3:1).

Yield 67%, m.p. = 234–235 °C. IR (KBr): 3321, 3237 (N-H), 1711, 1676 $cm^{-1}$ (C = O). $^1H$ NMR (δ/ppm): 2.25 (s, 3H, $CH_3$), 3.15 (s, 3H, $CH_3$), 4.14 (s, 2H, $CH_2$), 4.74 (s, 2H, $CH_2$), 7.10 (d, $J$ = 8.00 Hz, 2H, Ar-H), 7.32–7.54 (m, 5H, Ar-H), 7.78 (d, $J$ = 8.00 Hz, 2H, Ar-H), 8.17 (s, 1H, CH = N), 10.69 (s, 1H, NH), 11.84 (s, 1H, NH). $^{13}C$ NMR (δ/ppm): 12.47, 34.94, 35.43, 67.14, 108.31, 115.08 (2C), 123.80 (2C), 124.21, 126.43, 129.16 (2C), 129.87 (2C), 134.11, 136.52, 148.94, 159.70, 160.85, 163.05, 167.70, 177.59. MS $m/z$ (%): 478 ($M^+$, 62.73). Analysis for $C_{23}H_{22}N_6O_4S$ (478.14): Calcd: C, 57.73; H, 4.63; N, 17.56%. Found: C, 57.60; H, 4.69; N, 17.64%.

*2.1.5. Synthesis of N-(4-antipyrinyl)-2-(4-((2-(5-(4-chlorobenzylidene)-4-oxo-4,5-dihydrothiazol-2-yl)hydrazono) methyl)-phenoxy)acetamide (**6**):*

In a 100 mL round-bottom flask, 4-chlorobenzaldehyde (0.28 g, 2 mmol) and 0.10 mL piperidine were added to a solution of thiazolinone compound **5** (0.95 g, 2 mmol) in 35 mL ethanol. The mixture was refluxed for 2 h and then allowed to cool. The solid that formed was collected and washed with cold ethanol and dried.

Yield 83%, m.p. = 271–272 °C. IR (KBr): 3316, 3267 (N-H), 1693, 1675 $cm^{-1}$ (C = O). $^1H$ NMR (δ/ppm): 2.23 (s, 3H, $CH_3$), 3.18 (s, 3H, $CH_3$), 4.65 (s, 2H, $CH_2$), 7.11 (d, $J$ = 8.50 Hz, Ar-H), 7.27–7.64 (m, 9H, Ar-H), 7.78 (d, $J$ = 8.50 Hz, 2H, Ar-H), 7.97 (s, 1H, CH = C), 8.25 (s, 1H, CH = N), 10.35 (s, 1H, NH), 11.63 (s, 1H, NH). $^{13}C$ NMR (δ/ppm): 12.45, 35.51, 67.15, 108.56, 114.98 (2C), 123.83 (2C), 124.20, 126.40, 128.87 (2C), 129.13 (2C), 129.44 (2C), 129.90 (2C), 131.88, 133.10, 133.94, 134.45, 136.59, 146.07, 148.91, 159.74, 160.81, 161.94, 167.72, 171.05. MS $m/z$ (%): 602 ($M^+$ + 2, 16.38), 600 ($M^+$, 52.19). Analysis for $C_{30}H_{25}ClN_6O_4S$ (600.13): Calcd: C, 59.95; H, 4.19; N, 13.98%. Found: C, 59.76; H, 4.11; N, 13.85%.

*2.1.6. Synthesis of antipyrine-thiazole hybrids **7** and **8***

A 100 mL round-bottom flask was charged with a solution of thiosemicarbazone compound **3** (1.31 g, 3 mmol) in 40 mL ethanol and 0.2 mL triethylamine. Then, 3-chloroacetylacetone (0.39 mL, 3 mmol) and/or ethyl 4-chloroacetoacetate (0.48 mL, 3 mmol) was added and the mixture was refluxed for 4 h. The crude solid product that formed upon cooling was collected, dried and recrystallized from tetrahydrofuran to produce the targeted antipyrine-thiazole hybrids **7** and **8**, respectively.

*2.1.6.1. N-(4-Antipyrinyl)-2-(4-((2-(5-acetyl-4-methylthiazol-2-yl)hydrazono)methyl)phenoxy)-acetamide (**7**):*. Yield 62%, m.p. = 266–267 °C. IR (KBr): 3281, 3216 (N-H), broad at 1684 $cm^{-1}$ (C = O). $^1H$ NMR (δ/ppm): 2.27 (s, 3H, $CH_3$), 2.54 (s, 3H, $COCH_3$), 2.70 (s, 3H, $CH_3$), 3.21 (s, 3H, $CH_3$), 4.67 (s, 2H, $CH_2$), 7.10 (d, $J$ = 9.00 Hz, 2H, Ar-H), 7.28–7.50 (m, 5H, Ar-H), 7.77 (d, $J$ = 9.00 Hz, 2H, Ar-H), 8.04 (s, 1H, CH = N), 10.68 (s, 1H, NH), 11.75 (s, 1H, NH). $^{13}C$ NMR (δ/ppm): 12.46, 16.54, 27.03, 35.48, 67.13, 108.77, 114.06 (2C), 123.80 (2C), 124.17, 126.39, 126.86, 129.10 (2C), 129.92 (2C), 134.11, 136.62, 145.16, 155.08, 159.77, 160.83, 165.44, 167.65, 194.79. MS $m/z$ (%): 518 ($M^+$, 25.39). Analysis

for $C_{26}H_{26}N_6O_4S$ (518.17): Calcd: C, 60.22; H, 5.05; N, 16.21%. Found: C, 60.40; H, 5.14; N, 16.09%.

*2.1.6.2. Ethyl 2-(2-(2-(4-(2-((4-antipyrinyl)amino)-2-oxoethoxy)benzylidene)-hydrazinyl)thiazol-4-yl)acetate (**8**):.* Yield 58%, m.p. = 239–240 °C. IR (KBr): 3275, 3180 (N-H), 1727 (C = O), 1681 $cm^{-1}$ (C = O). $^1H$ NMR (δ/ppm): 1.23 (t, $J$ = 7.00 Hz, 3H), 2.25 (s, 3H, $CH_3$), 3.22 (s, 3H, $CH_3$), 4.18 (q, $J$ = 7.00 Hz, 2H), 4.74 (s, 2H, $CH_2$), 6.43 (s, 1H, thiazole-H5), 7.14 (d, $J$ = 8.00 Hz, 2H, Ar-H), 7.31–7.50 (m, 5H, Ar-H), 7.82 (d, $J$ = 8.00 Hz, 2H, Ar-H), 8.06 (s, 1H, CH = N), 10.62 (s, 1H, NH), 11.54 (s, 1H, NH). $^{13}C$ NMR (δ/ppm): 12.35, 14.37, 34.91, 35.37, 61.22, 67.11, 103.09, 109.04, 114.94 (2C), 123.48 (2C), 123.89, 126.46, 129.27 (2C), 129.88 (2C), 134.25, 137.30, 144.13, 145.80, 160.04, 160.58, 166.71, 167.52, 169.14. MS $m/z$ (%): 548 ($M^+$, 43.80). Analysis for $C_{27}H_{28}N_6O_5S$ (548.18): Calcd: C, 59.11; H, 5.14; N, 15.32%. Found: C, 58.92; H, 5.21; N, 15.41%.

### 2.2. Computational studies

The Gaussian 09 W program (Frisch et al., 2009) was used for optimize the geometry of the investigated compounds at DFT/B3LYP level with standard 6–311$^{++}$G(d,p) basis set (Becke, 1993, Lee et al., 1988, Perdew and Wang, 1992). The calculated frequencies for all compounds exhibited positive values confirming the stability of the optimized geometries. The DMol3 module implemented in the Materials Studio package (Biovia, 2017) was utilized in Fukui indices calculation using the gradient-corrected functional method (GGA) with a double numeric plus polarization (DNP) basis set (version 3.5) and B3LYP functional (Delley, 2006).

### 2.3. Biological activity

#### 2.3.1. Antibacterial screening

The synthesized antipyrine-thiazole hybrids were screened by inhibition zones method bacterial cultures as mentioned in supplementary file.

#### 2.3.2. Minimum inhibitory concentration testing

Minimal inhibitory concentration (MIC) values of antipyrinyl-thiazole derivatives were specified using disc agar dilution bacterial cultures recorded (Al-Anazi et al., 2019). See supplementary file.

#### 2.3.3. Antifungal activity

Dynamic inoculum technique has been applied on the synthesized antipyrine-thiazole derivatives and explained in the supplementary file.

### 2.4. Molecular docking

Docking theoeritical study was applied on the synthesized antipyrinyl-thiazole hybrids to determine their binding mode against disparate binding sites of *Staphylococcus aureus* "Homo sapiens" (PDB: 3HUN) protein (Tota and Battu, 2018). The synthesized hybrids were elected and then supplied using MOE operation "v10.2015.10".

## 3. Results and discussion

### 3.1. Synthesis of antipyrine-thiazole hybrids

The key of the present research, *N*-(4-antipyrinyl)-2-(4-formyl phenoxy)acetamide (**2**), was synthesized in 78% yield by reacting *N*-(4-antipyrinyl)-2-chloroacetamide (**1**) with 4-hydroxybenzaldehyde. The reaction proceeded by stirring in DMSO containing potassium carbonate to achieve the nucleophilic substitution of the chlorine atom from the *N*-(4-antipyrinyl)-2-chloroacetamide (**1**) by oxygen nucleophile of hydroxybenzaldehyde (Scheme 1). The key, *N*-(4-antipyrinyl)-2-(4-formylphenoxy)acetamide (**2**), was employed for the construction of antipyrine-thiazole hybrids via formation of various thiazole ring systems at the formylphenoxy moiety. Therefore, the synthetic strategy starts by condensation of the formyl group from the key **2** with thiosemicarbazide. The condensation was carried out by boiling in ethanol and glacial acetic acid to furnish the conforming thiosemicarbazone derivative **3**. The proposed structures of *N*-(4-antipyrinyl)-2-(4-formylphenoxy)acetamide **(2)** and its corresponding thiosemicarbazone derivative **3** were supported by the compatible elemental and spectral analyses.

The first antipyrine-thiazole compound **4** was produced by treating equimolar quantities of thiosemicarbazone compound **3** with 4-chlorophenacyl bromide in refluxing ethanol and triethylamine (Hantzsch-type reaction). The structure of antipyrine-thiazole hybrid **4** was inferred from its agreement spectral analyses (IR, $^1H$ NMR, $^{13}C$ NMR and mass analyses). Heterocyclization of thiosemicarbazone derivative **3** with ethyl bromoacetate has been achieved in boiling ethanol and sodium acetate to yield *N*-(4-antipyrinyl)-2-(4-((2-(4-oxothiazolin-2-yl)hydrazono)methyl)phenoxy)acetamide (**5**). The reactivity of cyclic methylene group (thiazolin-4-one ring system) of antipyrine-thiazole hybrid **5** proved to be reactive towards Knoevenagel condensation with 4-chlorobenzaldehyde (as an example). Such condensation was carried out by refluxing the reactants in ethanol and piperidine to furnish the corresponding 5-(4-chlorobenzylidene)-thiazolin-4-one derivative **6** (Scheme 2). The structures of antipyrine-thiazole hybrids **5** and **6** were secured based on their correct spectral analyses. For example, the IR spectrum of hybrid **6** demonstrated absorptions of the N-H groups at 3316 and 3267 $cm^{-1}$. While absorptions of the two carbonyl groups (C = O) were recorded at 1693 and 1675 $cm^{-1}$. The $^1H$ NMR spectrum displayed three singlet signals at δ 2.23, 3.18 and 4.65 ppm for the protons of two methyl groups and one methylene group, respectively. The aromatic protons were recorded doublet and multiplet signals in the region from δ 7.11 to 7.78 ppm. The olefinic (CH = C) and methine (CH = N) protons were observed as singlet signals at δ 7.97 and 8.25 ppm. The protons of NH groups resonate as singlet signals at δ 10.35 and 11.63 ppm. The mass spectrum exhibited the molecular ion peak at $m/z$ = 600 ($M^+$) and isotopic peak [$M^+$ + 2] at $m/z$ = 602 in the approximately ratio of 3:1, which supported a molecular formula ($C_{30}H_{25}ClN_6O_4S$).

The synthesis of antipyrine-thiazole hybrids **7** and **8** was achieved applying the Hantzsch-type reaction of thiosemicarbazone compound **3** with 3-chloroacetylacetone and/or ethyl 4-chloroacetoacetate in refluxing ethanol and triethylamine (Scheme 3). The structures of antipyrine-thiazole hybrids **7**

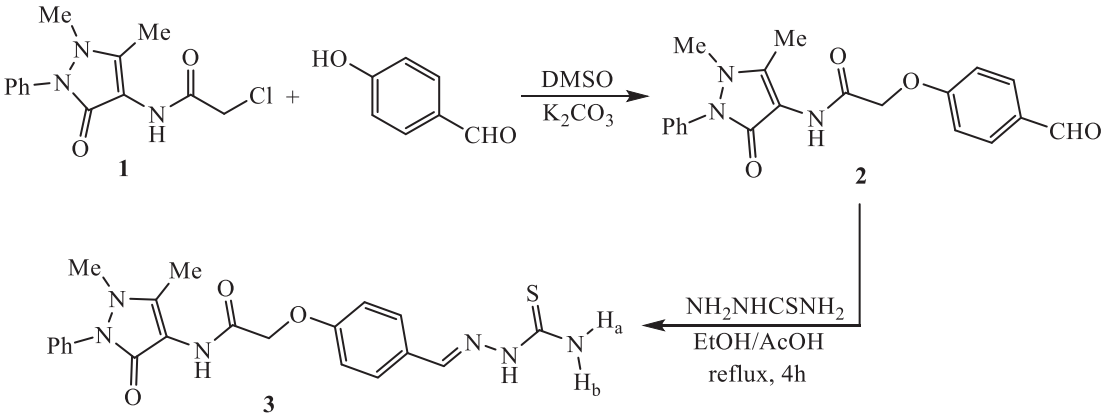


**Scheme 1**

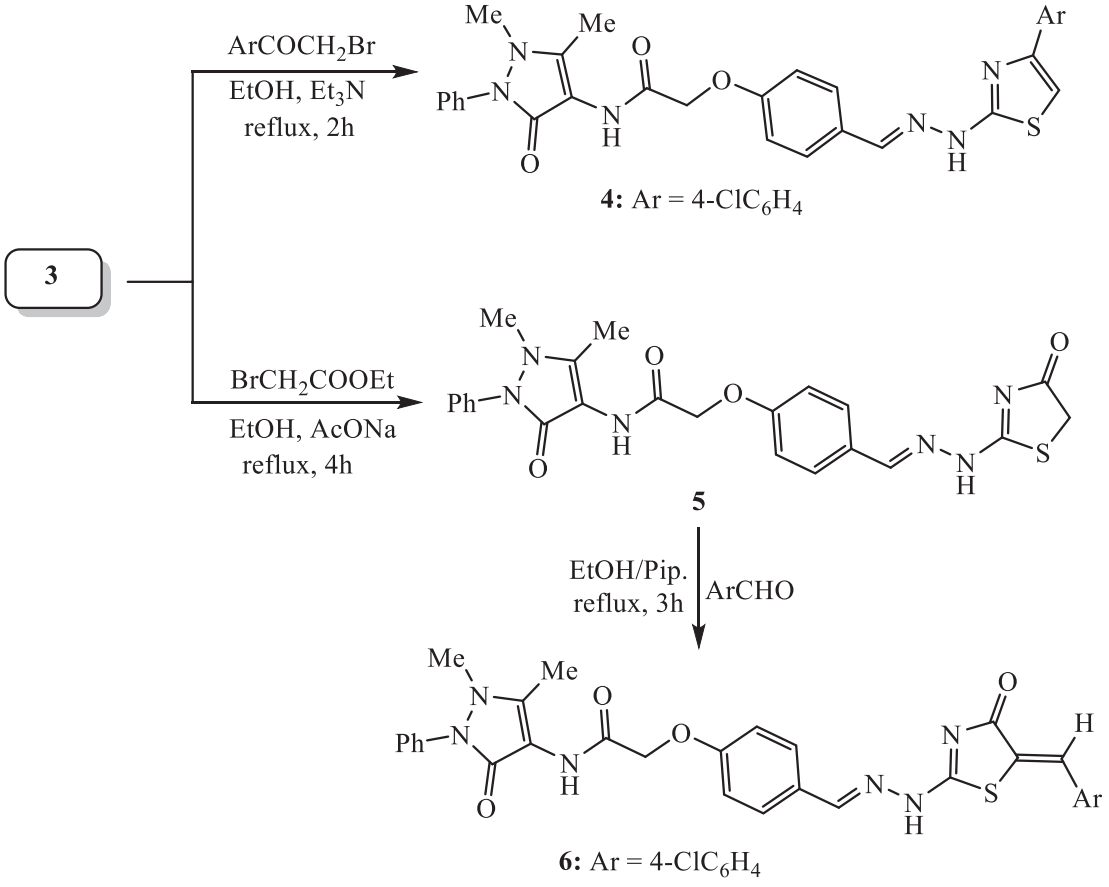


**Scheme 2**

and **8** were confirmed because of their agreement spectroscopic analyses. The IR spectrum of antipyrine-thiazole hybrid **8** demonstrated the absorptions of N-H functions at 3275 and 3180 $cm^{-1}$ as well as the absorption bands at 1727 and 1681 $cm^{-1}$ for the carbonyl groups. Moreover, $^1H$ NMR spectrum of showed the characteristic signal for the proton at fifth position of thiazole as singlet at $\delta$ 6.43 ppm. The other expected and characteristic signals are described in the experimental section.

### *3.2. DFT structural and electronic features*

The DFT optimized dihedral angle data of compounds **2** and **3**, shown in Fig. 2, indicated that both have almost coincided configuration except that the phenyl group at position 2 of the pyrazolyl ring was altered where $N_{Py1}$-$N_{Py2}$-$C^1_{Ph(Py2)}$-$C^2_{Ph(Py2)}$ was −5.72° and 171.27° in **2** and **3**, respectively (Tables S1, S2 and S3).

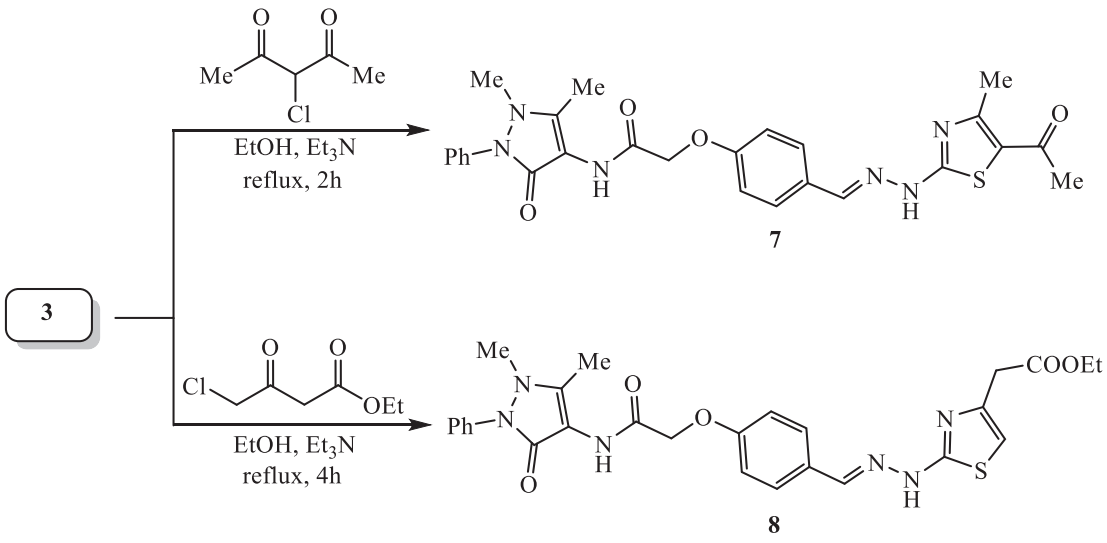


**Scheme 3**

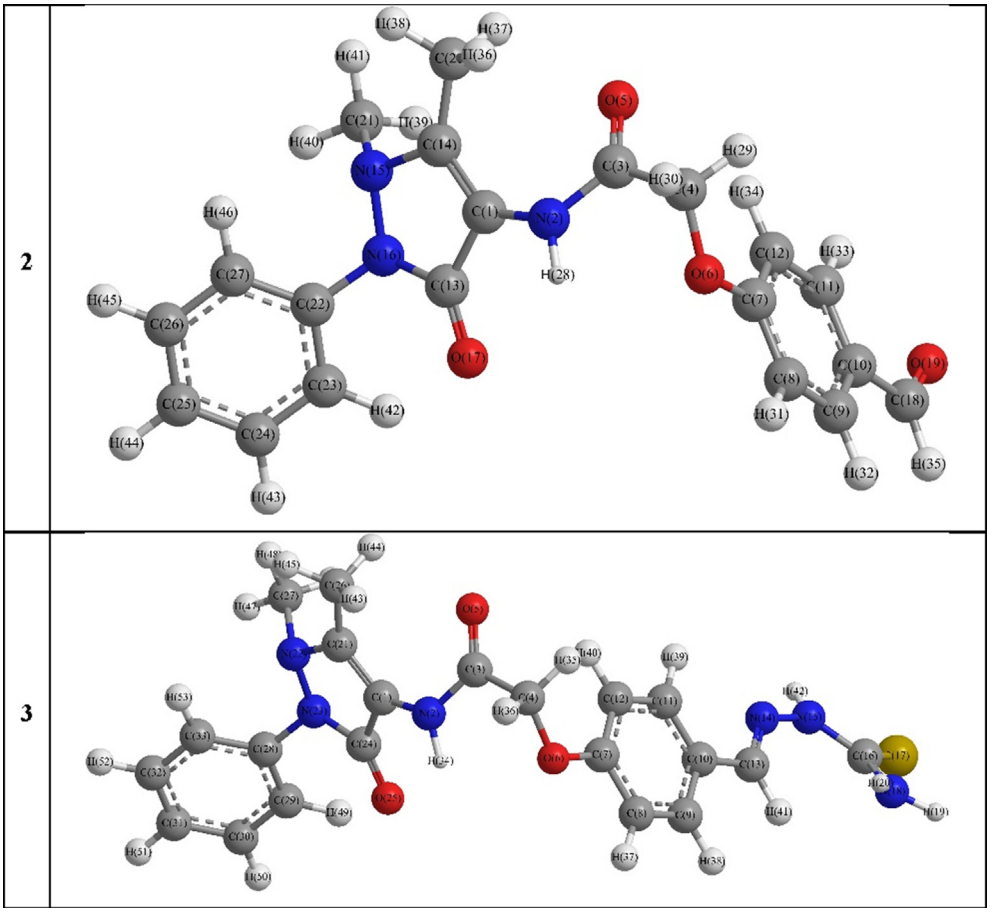


**Fig. 2** DFT Optimized structures of compounds **2** and **3**.

The optimized structural data of the **4**–**6** derivatives showed that compound **5** has dissimilar configuration with respect to the other compounds (Fig. 3). For example, the pyrazolyl moiety became more planar while its phenyl substituent was almost perpendicular on its plane, i.e., $C_{Py4}$-$C_{Py3}$-$N_{Py2}$-$N_{Py1}$ was −9.46, 3.24 and −9.44°; $N_{Py1}$-$N_{Py2}$-$C^1_{Ph(Py2)}$-$C^2_{Ph(Py2)}$ was 171.37, 109.33 and 171.34° for compounds **4**, **5** and **6**, respectively (Tables S1, S2 and S3). Also, the acetamide carbonyl group position was strongly altered where $C_{Py3}$-$C_{Py4}$-$NH_{(Act)}$–$CO_{(Act)}$ and $C_{Py4}$-$NH_{(Act)}$–$CO_{(Act)}$–$OC_{(Act)}$ were

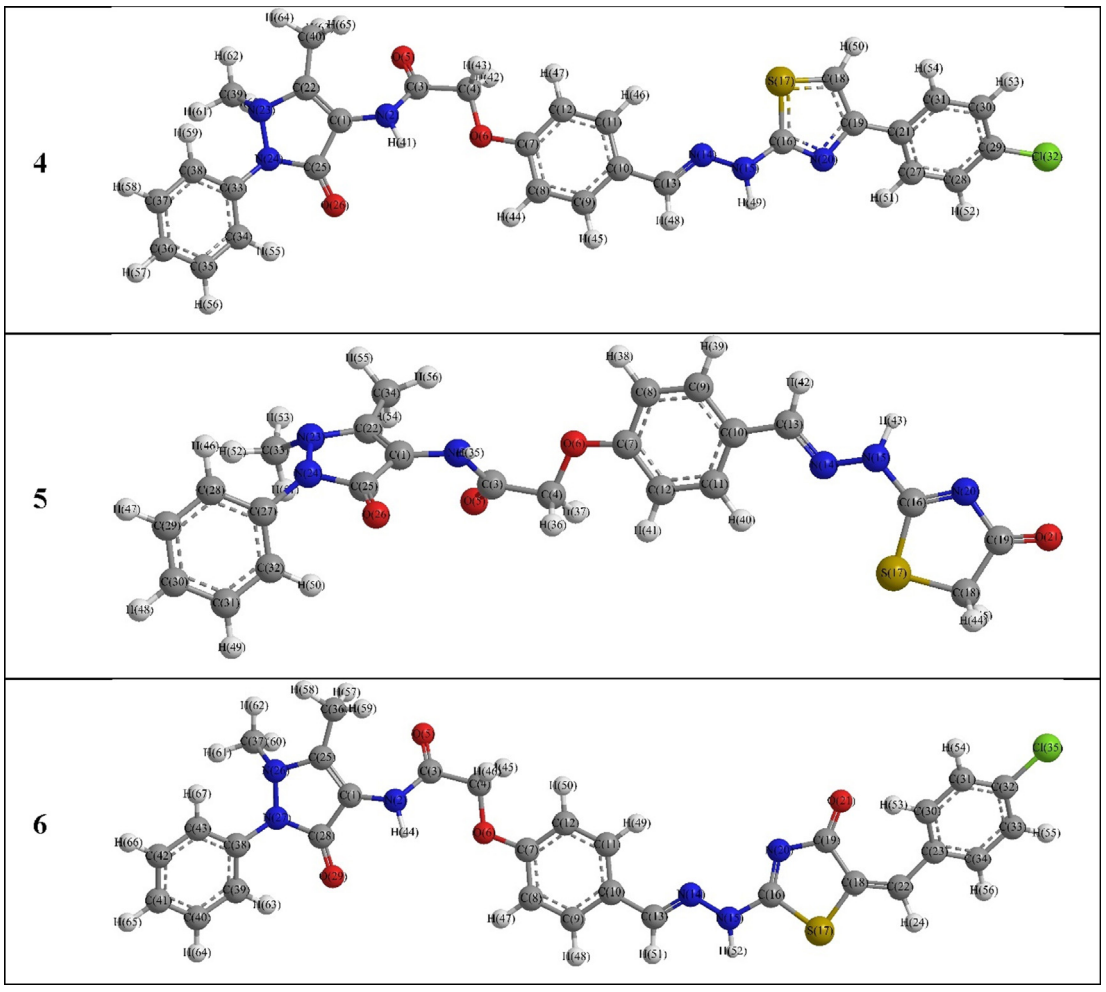


**Fig. 3** DFT Optimized structures of the **4**–**6** derivatives.

138.1 and 12.4°, in both **4** and **6**, while 103.5 and 20.2° were observed in **5** derivative. Furthermore, the orientation of the planar thiazole ring was different in these derivatives, e.g., the $C_{Hz}$-$N^1_{Hz}$-$N^2_{Hz}$-$C_{thia2}$ = 159.00, −173.33 and 164.48°; $N^1_{Hz}$-$N^2_{Hz}$-$C_{thia2}$-$S_{thia1}$ = 47.53, −26.55 and −176.76°, for **4**, **5** and **6**, respectively.

The derivatives **7** and **8** structural data indicated that both have almost coincided configuration with each other and close to that of compound **6** (Fig. 4). They showed changed orientation of the thiazole ring with respect to the hydrazone carbon and nitrogen atoms where the $C_{Hz}$-$N^1_{Hz}$-$N^2_{Hz}$-$C_{thia2}$ = 161.51 and −159.02°; and $N^1_{Hz}$-$N^2_{Hz}$-$C_{thia2}$-$S_{thia1}$ = 38.05 and −46.42°, for **7** and **8** compounds, respectively (Tables S1, S2 and S3). Moreover, the acetyl and methyl groups in **7** was slightly shifted down the thiazole ring plane, i.e., $S_{thia1}$-$C_{thia5}$-$CO_{Ac(thia5)}$-$OC_{Ac(thia5)}$ and $CO_{Ac(thia5)}$-$C_{thia5}$-$C_{thia4}$-$C_{Me(thia4)}$ were −176.92 and 0.33°, respectively. On the other hand, the carbonyl carbon of the ester group in compound 8 was lied below the thiazole plane while their oxygen atoms were positioned in two different planes, i.e., $N_{thia3}$-$C_{thia4}$-$CH_{2(thia4)}$-$COOEt_{(thia4)}$ = -43.10°, $C_{thia4}$-$CH_{2(thia4)}$-$COOEt_{(thia4)}$-$O^1COEt_{(thia4)}$ = 111.53° and $C_{thia4}$-$CH_{2(thia4)}$-$COOEt_{(thia4)}$-$O^2COEt_{(thia4)}$ = -70.99°.

Lastly, the bond length and angle data were almost agreed with those obtained from single crystal x-ray of comparable compounds, where the DFT lengths were longer than the corresponding x-ray by only 0.06–0.19 Å (Bakir et al., 2020, Bakir, 2018, Bakir et al., 2016, Bakir et al., 2004, Benassi et al., 1989, Distefano et al., 1998), where the quantum chemical calculations have no intermolecular columbic interactions as it carried out for isolated molecule in gaseous state, while the experimental belong to the molecules in solid state interacting in crystal lattice (Sajan et al., 2011) (Tables S1-S3).

### *3.2.1. Frontier molecular orbitals*

The HOMO-LUMO configuration and energy values account for the molecule ability to donate or accept electrons (Bulat et al., 2004). The molecules with low HOMO-LUMO energy gap processes feasible intramolecular charge transfer (Xavier et al., 2015, Makhlouf et al., 2018) which may affect the molecule's bioactivity (Bouchoucha et al., 2018). The 3D representations of the investigated compounds frontier molecular orbitals were presented in Fig. 5. The plots designated that compound **2** has HOMO centered on the phenylpyrazolone moiety while its LUMO was mainly spread over the benzaldehyde group. Likewise, the HOMO of compounds **5** and **6** were consisted of the π-orbital of phenylpyrazolone and heteroatoms lone pair of electrons whereas the π*-orbitals of benzylidenehydrazineyl thiazolone group involved in formation of the LUMO. Alternatively, the compound **3**, **4** and **8** showed differ-

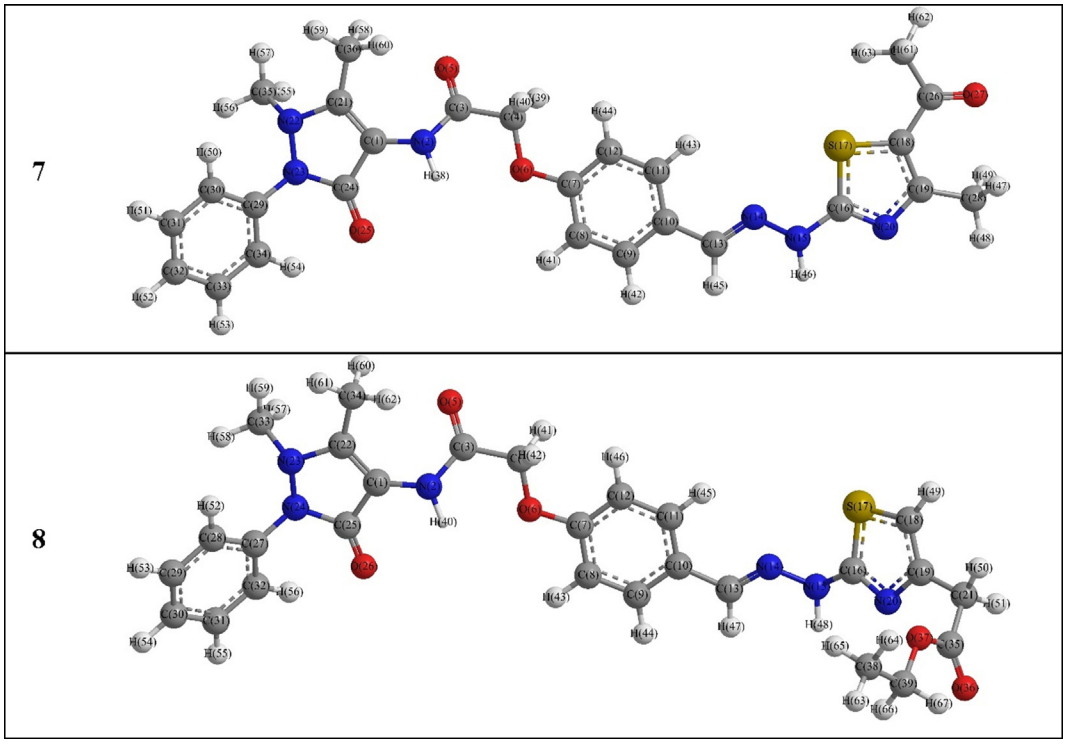


**Fig. 4** DFT Optimized structures of the **7**–**8** derivatives.

ent behavior in which the HOMO and LUMO were consisted of the π- and π*-orbitals, respectively, of the benzylidenehydrazineyl thiazole moiety (Fig. 5).

As shown in Table 1, the energy of HOMO and LUMO, $E_H$ and $E_L$, respectively, were affected by the abovementioned foundations. Thus, the data showed that compounds **3** and **8** have the lowest $E_H$ and $E_L$ values, −5.73 and −3.05 eV, respectively. On contrary, the energy gap ($\Delta E_{H\text{-}L}$) data revealed that compound **6** has the lowest value, 1.94 eV, while compound **8** has the highest, 2.71 eV. Hence, the investigated compounds may be ranked due to their energy gap as following **6** < **5** < **7** < **3** < **2** < **4** < **8**.

In addition, the $E_{HOMO}$ and $E_{LUMO}$ were exploited in some chemical reactivity descriptors estimation like electronegativity (χ), global hardness (η), softness (δ) and electrophilicity (ω), using the following formulae (Xavier et al., 2015).

$$\chi = -\frac{1}{2}(E_{HOMO} + E_{LUMO})\eta = -\frac{1}{2}(E_{HOMO} - E_{LUMO})$$

$$\delta = \frac{1}{\eta}\omega = \frac{\chi^2}{2\eta}$$

Finally, Table 1 data showed that compound **6** has the highest Lewis's acid character and charge transfer ability, due to electronegativity (χ) and global softness (δ) values, respectively. On contrary, compound 8 has the lowest Lewis's acid character and charge transfer ability but the highest global hardness (η). Thus, according to softness, the investigated derivatives were ordered as **8** < **4** < **2** < **3** < **7** < **5** < **6**, which the reversed order due to their energy gap ($\Delta E_{H\text{-}L}$).

*3.2.2. Atomic Mulliken's charges and Fukui's indices*

The molecules electronegativity and charge transfer processes can be understood from the DFT Mulliken's atomic charges (Bhagyasree et al., 2013) (Table 2). In all compounds, both of oxygen and nitrogen atoms have negative Mulliken's charge, −0.414 - −0.460 and −0.057 - −0.552, respectively. Whereas, the sulfur atom, that has negative charge in thiosemicarbazone compound **3**, −0.243, turned to be positively charged when involved in thiazole ring formation in compounds **4**–**8**, +0.163 - +0.312, which may be attributed to strong involvement of their lone pair of electrons in resonating structure of the thiadiazole ring. In accordance, the pyrazolone nitrogen atoms, $N_{Py1}$ and $N_{Py2}$, have lower negative charge than the thiazole one, $N_{thia3}$, −0.176 - −0.247 and −0.261 - −0.298, respectively. Moreover, the acetamide nitrogen, $NH_{(Act)}$, showed higher negative charge than the hydrazinic nitrogen atoms, $N^1_{Hz}$ and $H^2_{Hz}$, which clear the electron release effect of the pyrazolone ring. On the other hand, the data showed that all oxygen atoms have close negative charge, −0.414 - −0.460, which may be attributed to the strong electronegativity of the oxygen atoms.

The Fukui's indices of atomic reactivity toward nucleophilic, electrophilic and radical attacks, $f_k^+$, $f_k^-$ and $f_k^0$, respectively, were evaluated (Olasunkanmi et al., 2016, El Adnani et al., 2013, Mi et al., 2015, Messali et al., 2018). The Fukui's indices ($f_k^+$) data demonstrated different pattern of the most susceptible atoms for nucleophilic attack. For instance, the hydrazinic carbon and nitrogen atoms, $C_{Hz}$ and $N^1_{Hz}$, respectively, appeared among the top three susceptible sites in compounds **3**–**8** while in **2** the highly liable atoms were Likewise,

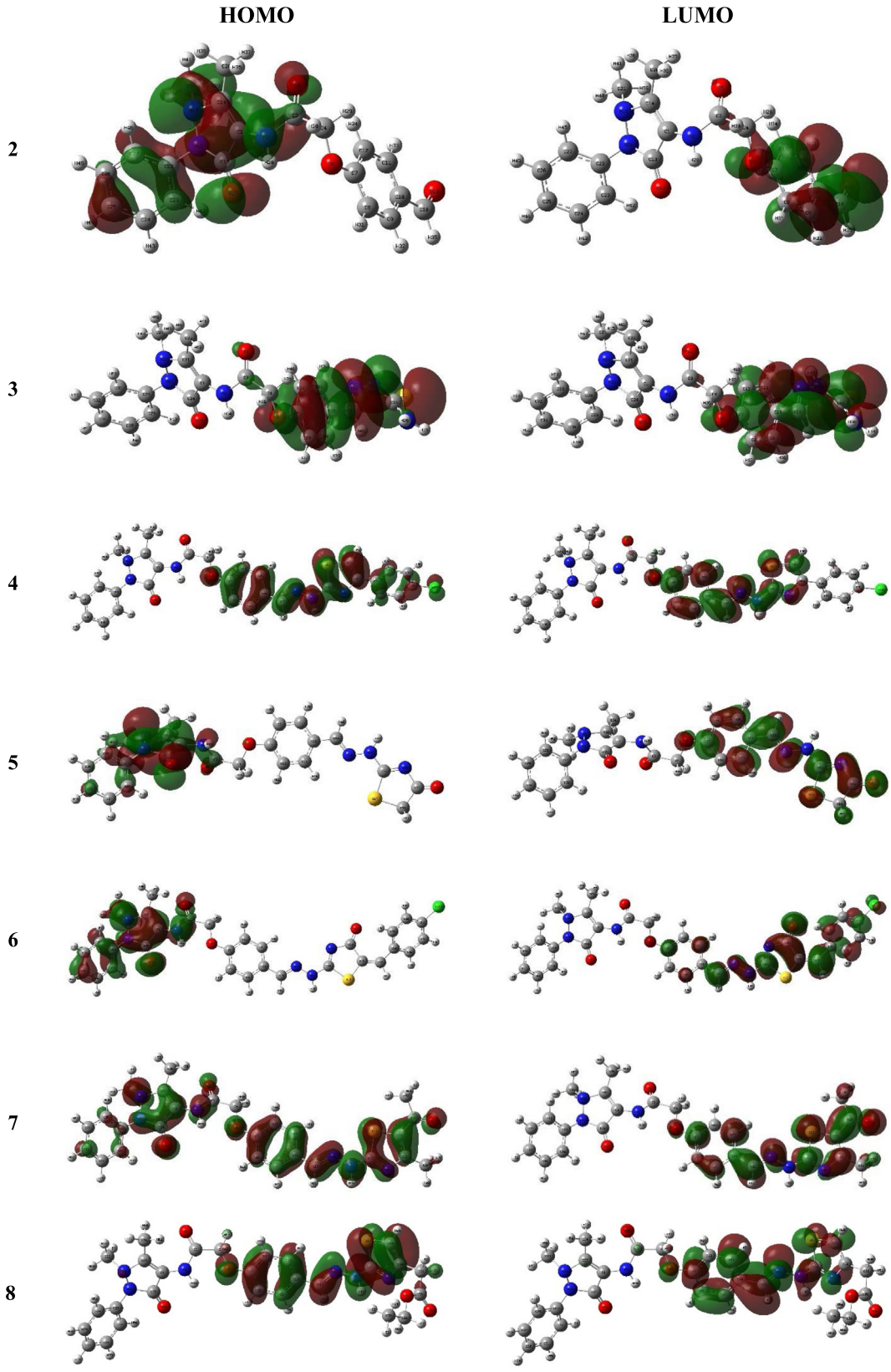


**Fig. 5** The frontier molecular orbital of compounds **4a-c** and **5a-c**.

**Table 1** The HOMO-LUMO energies and chemical reactivity descriptors (eV) of investigated compounds.

| Compound | $E_H$ | $E_L$ | $\Delta E_{H-L}$ | $\chi$ | $\eta$ | $\delta$ | $\omega$ |
|---|---|---|---|---|---|---|---|
| **2** | −6.01 | −3.41 | 2.60 | 4.71 | 1.30 | 0.77 | 8.54 |
| **3** | −5.73 | −3.18 | 2.54 | 4.46 | 1.27 | 0.79 | 7.80 |
| **4** | −5.75 | −3.09 | 2.66 | 4.42 | 1.33 | 0.75 | 7.34 |
| **5** | −5.82 | −3.50 | 2.32 | 4.66 | 1.16 | 0.86 | 9.33 |
| **6** | −5.94 | −4.00 | 1.94 | 4.97 | 0.97 | 1.03 | 12.71 |
| **7** | −5.94 | −3.49 | 2.45 | 4.72 | 1.22 | 0.82 | 9.10 |
| **8** | −5.76 | −3.05 | 2.71 | 4.40 | 1.36 | 0.74 | 7.16 |

**Table 2** The Mulliken's atomic charges (a.u.) of investigated compounds.

| Atom | 2 | 3 | 4 | 5 | 6 | 7 | 8 |
|---|---|---|---|---|---|---|---|
| $N_{Py1}$ | −0.176 | −0.186 | −0.187 | −0.187 | −0.187 | −0.186 | −0.187 |
| $N_{Py2}$ | −0.195 | −0.219 | −0.218 | −0.247 | −0.218 | −0.218 | −0.218 |
| $C_{Py3}$ | 0.375 | 0.375 | 0.375 | 0.360 | 0.374 | 0.374 | 0.373 |
| $C_{Py4}$ | 0.140 | 0.143 | 0.141 | 0.120 | 0.141 | 0.141 | 0.141 |
| $C_{Py5}$ | 0.210 | 0.236 | 0.235 | 0.274 | 0.237 | 0.236 | 0.237 |
| $O_{(Py3)}$ | −0.458 | −0.450 | −0.453 | −0.443 | −0.453 | −0.453 | −0.452 |
| $C^1_{Ph(Py2)}$ | 0.244 | 0.249 | 0.249 | 0.253 | 0.249 | 0.249 | 0.249 |
| $C_{Me(Py1)}$ | −0.441 | −0.519 | −0.518 | −0.527 | −0.519 | −0.519 | −0.519 |
| $C_{Me(Py5)}$ | −0.628 | −0.722 | −0.722 | −0.728 | −0.722 | −0.722 | −0.722 |
| $NH_{(Act)}$ | −0.486 | −0.511 | −0.518 | −0.552 | −0.518 | −0.518 | −0.518 |
| $CO_{(Act)}$ | 0.442 | 0.447 | 0.474 | 0.482 | 0.474 | 0.475 | 0.474 |
| $OC_{(Act)}$ | −0.457 | −0.457 | −0.454 | −0.414 | −0.453 | −0.454 | −0.455 |
| $CH_{2(Act)}$ | −0.214 | −0.272 | −0.273 | −0.279 | −0.275 | −0.274 | −0.273 |
| $O_{(Ph)}$ | −0.456 | −0.458 | −0.460 | −0.438 | −0.457 | −0.458 | −0.460 |
| $C^1_{Ph}$ | 0.407 | 0.387 | 0.399 | 0.399 | 0.404 | 0.401 | 0.399 |
| $C^4_{Ph}$ | 0.149 | 0.202 | 0.199 | 0.197 | 0.198 | 0.198 | 0.200 |
| CHO | 0.078 | | | | | | |
| OCH | −0.364 | | | | | | |
| $C_{Hz}$ | | −0.252 | −0.217 | −0.195 | −0.205 | −0.213 | −0.217 |
| $N^1_{Hz}$ | | −0.086 | −0.095 | −0.111 | −0.057 | −0.096 | −0.095 |
| $N^2_{Hz}$ | | −0.332 | −0.362 | −0.348 | −0.345 | −0.351 | −0.360 |
| $CS_{Hz}$ | | 0.230 | | | | | |
| $SC_{Hz}$ | | −0.243 | | | | | |
| $NH_{2Hz}$ | | −0.673 | | | | | |
| $S_{thia1}$ | | | 0.312 | 0.175 | 0.163 | 0.291 | 0.305 |
| $C_{thia2}$ | | | 0.089 | 0.145 | 0.132 | 0.097 | 0.096 |
| $N_{thia3}$ | | | −0.280 | −0.298 | −0.261 | −0.272 | −0.271 |
| $C_{thia4}$ | | | 0.220 | 0.438 | 0.381 | 0.268 | 0.303 |
| $C_{thia5}$ | | | −0.500 | −0.632 | −0.129 | −0.227 | −0.481 |
| $C^1_{Ph(thia)}$ | | | 0.159 | | | | |
| $C^4_{Ph(thia)}$ | | | 0.178 | | | | |
| Cl | | | −0.173 | | | | |
| $O_{(thia4)}$ | | | | −0.362 | −0.397 | | |
| $CH_{(Bz)}$ | | | | | −0.242 | | |
| $C^1_{Ph(Bz)}$ | | | | | 0.193 | | |
| $C^4_{Ph(Bz)}$ | | | | | 0.185 | | |
| Cl | | | | | −0.164 | | |
| $CMe_{(thia4)}$ | | | | | | −0.690 | |
| $CO_{Ac(thia5)}$ | | | | | | 0.387 | |
| $OC_{Ac(thia5)}$ | | | | | | −0.426 | |
| $CMe_{Ac(thia5)}$ | | | | | | −0.727 | |
| $CH_{2(thia4)}$ | | | | | | | −0.577 |
| $COOEt_{(thia4)}$ | | | | | | | 0.584 |
| $O^1COEt_{(thia4)}$ | | | | | | | −0.425 |
| $O^2COEt_{(thia4)}$ | | | | | | | −0.421 |
| $CEt_{(thia4)}$ | | | | | | | −0.126 |

**Table 3** The Fukui's indices and relative electrophilicity and nucleophilicity descriptors.

| Atom | $f_k^+$ | $f_k^-$ | $f_k^0$ | $s_k^+/s_k^-$ | $s_k^-/s_k^+$ | Atom | $f_k^+$ | $f_k^-$ | $f_k^0$ | $s_k^+/s_k^-$ | $s_k^-/s_k^+$ |
|---|---|---|---|---|---|---|---|---|---|---|---|
| **2** | | | | | | **3** | | | | | |
| $N_{Py1}$ | 0.010 | 0.075 | 0.042 | 0.13 | 7.50 | $N_{Py1}$ | 0.008 | 0.007 | 0.008 | 1.14 | 0.88 |
| $N_{Py2}$ | 0.003 | 0.052 | 0.027 | 0.06 | 17.33 | $N_{Py2}$ | 0.002 | 0.002 | 0.002 | 1.00 | 1.00 |
| $C_{Py3}$ | 0.002 | 0.042 | 0.020 | 0.05 | 21.00 | $C_{Py3}$ | 0.001 | 0.002 | 0.002 | 0.50 | 2.00 |
| $C_{Py4}$ | 0.006 | 0.054 | 0.024 | 0.11 | 9.00 | $C_{Py4}$ | 0.004 | 0.005 | 0.004 | 0.80 | 1.25 |
| $C_{Py5}$ | 0.009 | 0.028 | 0.019 | 0.32 | 3.11 | $C_{Py5}$ | 0.009 | 0.005 | 0.007 | 1.80 | 0.56 |
| $O_{(Py3)}$ | 0.007 | 0.115 | 0.054 | 0.06 | 16.43 | $O_{(Py3)}$ | 0.005 | 0.006 | 0.005 | 0.83 | 1.20 |
| $C^1_{Ph(Py2)}$ | 0.003 | 0.009 | 0.003 | 0.33 | 3.00 | $C^1_{Ph(Py2)}$ | 0.003 | 0.003 | 0.003 | 1.00 | 1.00 |
| $CMe_{(Py1)}$ | 0.004 | 0.024 | 0.014 | 0.17 | 6.00 | $CMe_{(Py1)}$ | 0.004 | 0.003 | 0.003 | 1.33 | 0.75 |
| $CMe_{(Py5)}$ | 0.003 | 0.011 | 0.007 | 0.27 | 3.67 | $CMe_{(Py5)}$ | 0.003 | 0.002 | 0.003 | 1.50 | 0.67 |
| $NH_{(Act)}$ | 0.004 | 0.027 | 0.015 | 0.15 | 6.75 | $NH_{(Act)}$ | 0.004 | 0.003 | 0.003 | 1.33 | 0.75 |
| $CO_{(Act)}$ | 0.005 | 0.026 | 0.010 | 0.19 | 5.20 | $CO_{(Act)}$ | 0.001 | 0.005 | 0.003 | 0.20 | 5.00 |
| $OC_{(Act)}$ | 0.015 | 0.043 | 0.029 | 0.35 | 2.87 | $OC_{(Act)}$ | 0.012 | 0.010 | 0.011 | 1.20 | 0.83 |
| $CH_{2(Act)}$ | 0.010 | 0.007 | 0.009 | 1.43 | 0.70 | $CH_{2(Act)}$ | 0.008 | 0.007 | 0.008 | 1.14 | 0.88 |
| $O_{(Ph)}$ | 0.045 | 0.002 | 0.021 | 22.50 | 0.04 | $O_{(Ph)}$ | 0.031 | 0.037 | 0.034 | 0.84 | 1.19 |
| $C^1_{Ph}$ | 0.077 | 0.009 | 0.034 | 8.56 | 0.12 | $C^1_{Ph}$ | 0.052 | 0.043 | 0.048 | 1.21 | 0.83 |
| $C^4_{Ph}$ | 0.037 | 0.007 | 0.022 | 5.29 | 0.19 | $C^4_{Ph}$ | 0.021 | 0.017 | 0.019 | 1.24 | 0.81 |
| $CHO_{(Ph)}$ | 0.146 | 0.008 | 0.077 | 18.25 | 0.05 | $C_{Hz}$ | 0.085 | 0.061 | 0.073 | 1.39 | 0.72 |
| $OCH_{(Ph)}$ | 0.153 | 0.016 | 0.084 | 9.56 | 0.10 | $N^1_{Hz}$ | 0.083 | 0.049 | 0.066 | 1.69 | 0.59 |
| | | | | | | $N^2_{Hz}$ | 0.026 | 0.059 | 0.042 | 0.44 | 2.27 |
| | | | | | | $CS_{Hz}$ | 0.042 | 0.028 | 0.035 | 1.50 | 0.67 |
| | | | | | | $SC_{Hz}$ | 0.169 | 0.288 | 0.229 | 0.59 | 1.70 |
| | | | | | | $NH_{2Hz}$ | 0.034 | 0.035 | 0.035 | 0.97 | 1.03 |
| **4** | | | | | | **5** | | | | | |
| **Atom** | $f_k^+$ | $f_k^-$ | $f_k^0$ | $s_k^+/s_k^-$ | $s_k^-/s_k^+$ | **Atom** | $f_k^+$ | $f_k^-$ | $f_k^0$ | $s_k^+/s_k^-$ | $s_k^-/s_k^+$ |
| $N_{Py1}$ | 0.008 | 0.006 | 0.007 | 1.33 | 0.75 | $N_{Py1}$ | 0.005 | 0.097 | 0.051 | 0.05 | 19.40 |
| $N_{Py2}$ | 0.004 | 0.003 | 0.004 | 1.33 | 0.75 | $N_{Py2}$ | 0.003 | 0.060 | 0.032 | 0.05 | 20.00 |
| $C_{Py3}$ | 0.001 | 0.000 | 0.001 | 0.00 | 0.00 | $C_{Py3}$ | 0.001 | 0.046 | 0.023 | 0.02 | 46.00 |
| $C_{Py4}$ | 0.001 | 0.002 | 0.002 | 0.50 | 2.00 | $C_{Py4}$ | 0.005 | 0.060 | 0.028 | 0.08 | 12.00 |
| $C_{Py5}$ | 0.011 | 0.004 | 0.007 | 2.75 | 0.36 | $C_{Py5}$ | 0.002 | 0.033 | 0.018 | 0.06 | 16.50 |
| $O_{(Py3)}$ | 0.000 | 0.002 | 0.001 | 0.00 | 0.00 | $O_{(Py3)}$ | 0.002 | 0.138 | 0.068 | 0.01 | 69.00 |
| $C^1_{Ph(Py2)}$ | 0.002 | 0.002 | 0.002 | 1.00 | 1.00 | $C^1_{Ph(Py2)}$ | 0.002 | 0.009 | 0.006 | 0.22 | 4.50 |
| $CMe_{(Py1)}$ | 0.004 | 0.003 | 0.003 | 1.33 | 0.75 | $CMe_{(Py1)}$ | 0.003 | 0.028 | 0.016 | 0.11 | 9.33 |
| $CMe_{(Py5)}$ | 0.003 | 0.001 | 0.002 | 3.00 | 0.33 | $CMe_{(Py5)}$ | 0.001 | 0.013 | 0.007 | 0.08 | 13.00 |
| $NH_{(Act)}$ | 0.004 | 0.002 | 0.003 | 2.00 | 0.50 | $NH_{(Act)}$ | 0.001 | 0.015 | 0.008 | 0.07 | 15.00 |
| $CO_{(Act)}$ | 0.004 | 0.003 | 0.000 | 1.33 | 0.75 | $CO_{(Act)}$ | 0.002 | 0.017 | 0.007 | 0.12 | 8.50 |
| $OC_{(Act)}$ | 0.018 | 0.010 | 0.014 | 1.80 | 0.56 | $OC_{(Act)}$ | 0.015 | 0.025 | 0.020 | 0.60 | 1.67 |
| $CH_{2(Act)}$ | 0.008 | 0.005 | 0.006 | 1.60 | 0.63 | $CH_{2(Act)}$ | 0.007 | 0.005 | 0.006 | 1.40 | 0.71 |
| $O_{(Ph)}$ | 0.028 | 0.031 | 0.030 | 0.90 | 1.11 | $O_{(Ph)}$ | 0.033 | 0.004 | 0.015 | 8.25 | 0.12 |
| $C^1_{Ph}$ | 0.050 | 0.035 | 0.042 | 1.43 | 0.70 | $C^1_{Ph}$ | 0.053 | 0.004 | 0.025 | 13.25 | 0.08 |
| $C^4_{Ph}$ | 0.026 | 0.015 | 0.020 | 1.73 | 0.58 | $C^4_{Ph}$ | 0.021 | 0.011 | 0.016 | 1.91 | 0.52 |
| $C_{Hz}$ | 0.077 | 0.051 | 0.064 | 1.51 | 0.66 | $C_{Hz}$ | 0.094 | 0.004 | 0.049 | 23.50 | 0.04 |
| $N^1_{Hz}$ | 0.079 | 0.021 | 0.050 | 3.76 | 0.27 | $N^1_{Hz}$ | 0.074 | 0.013 | 0.043 | 5.69 | 0.18 |
| $N^2_{Hz}$ | 0.029 | 0.063 | 0.046 | 0.46 | 2.17 | $N^2_{Hz}$ | 0.022 | 0.009 | 0.015 | 2.44 | 0.41 |
| $S_{thia1}$ | 0.047 | 0.089 | 0.068 | 0.53 | 1.89 | $S_{thia1}$ | 0.060 | 0.003 | 0.032 | 20.00 | 0.05 |
| $C_{thia2}$ | 0.010 | 0.025 | 0.018 | 0.40 | 2.50 | $C_{thia2}$ | 0.041 | 0.002 | 0.022 | 20.50 | 0.05 |
| $N_{thia3}$ | 0.031 | 0.035 | 0.033 | 0.89 | 1.13 | $N_{thia3}$ | 0.044 | 0.011 | 0.027 | 4.00 | 0.25 |
| $C_{thia4}$ | 0.022 | 0.044 | 0.033 | 0.50 | 2.00 | $C_{thia4}$ | 0.043 | 0.006 | 0.024 | 7.17 | 0.14 |
| $C_{thia5}$ | 0.033 | 0.064 | 0.048 | 0.52 | 1.94 | $C_{thia5}$ | 0.018 | 0.004 | 0.011 | 4.50 | 0.22 |
| $C^1_{Ph(thia)}$ | 0.004 | 0.003 | 0.000 | 1.33 | 0.75 | $O_{(thia4)}$ | 0.076 | 0.016 | 0.046 | 4.75 | 0.21 |
| $C^4_{Ph(thia)}$ | 0.016 | 0.028 | 0.022 | 0.57 | 1.75 | | | | | | |
| Cl | 0.035 | 0.065 | 0.050 | 0.54 | 1.86 | | | | | | |
| **6** | | | | | | **7** | | | | | |
| **Atom** | $f_k^+$ | $f_k^-$ | $f_k^0$ | $s_k^+/s_k^-$ | $s_k^-/s_k^+$ | **Atom** | $f_k^+$ | $f_k^-$ | $f_k^0$ | $s_k^+/s_k^-$ | $s_k^-/s_k^+$ |
| $N_{Py1}$ | 0.004 | 0.041 | 0.022 | 0.10 | 10.25 | $N_{Py1}$ | 0.005 | 0.022 | 0.014 | 0.23 | 4.40 |
| $N_{Py2}$ | 0.002 | 0.025 | 0.013 | 0.08 | 12.50 | $N_{Py2}$ | 0.002 | 0.013 | 0.008 | 0.15 | 6.50 |
| $C_{Py3}$ | 0.001 | 0.020 | 0.010 | 0.05 | 20.00 | $C_{Py3}$ | 0.001 | 0.009 | 0.004 | 0.11 | 9.00 |
| $C_{Py4}$ | 0.003 | 0.027 | 0.012 | 0.11 | 9.00 | $C_{Py4}$ | 0.004 | 0.010 | 0.003 | 0.40 | 2.50 |
| $C_{Py5}$ | 0.003 | 0.016 | 0.010 | 0.19 | 5.33 | $C_{Py5}$ | 0.004 | 0.010 | 0.007 | 0.40 | 2.50 |
| $O_{(Py3)}$ | 0.003 | 0.056 | 0.026 | 0.05 | 18.67 | $O_{(Py3)}$ | 0.004 | 0.024 | 0.010 | 0.17 | 6.00 |
| $C^1_{Ph(Py2)}$ | 0.002 | 0.001 | 0.000 | 2.00 | 0.50 | $C^1_{Ph(Py2)}$ | 0.002 | 0.001 | 0.001 | 2.00 | 0.50 |
| $CMe_{(Py1)}$ | 0.002 | 0.013 | 0.008 | 0.15 | 6.50 | $CMe_{(Py1)}$ | 0.003 | 0.008 | 0.005 | 0.38 | 2.67 |

(*continued on next page*)

**Table 3** (*continued*)

| Atom | $f_k^+$ | $f_k^-$ | $f_k^0$ | $s_k^+/s_k^-$ | $s_k^-/s_k^+$ | Atom | $f_k^+$ | $f_k^-$ | $f_k^0$ | $s_k^+/s_k^-$ | $s_k^-/s_k^+$ |
|---|---|---|---|---|---|---|---|---|---|---|---|
| $CMe_{(Py5)}$ | 0.001 | 0.007 | 0.004 | 0.14 | 7.00 | $CMe_{(Py5)}$ | 0.001 | 0.004 | 0.003 | 0.25 | 4.00 |
| $NH_{(Act)}$ | 0.001 | 0.016 | 0.008 | 0.06 | 16.00 | $NH_{(Act)}$ | 0.001 | 0.008 | 0.005 | 0.13 | 8.00 |
| $CO_{(Act)}$ | 0.003 | 0.012 | 0.005 | 0.25 | 4.00 | $CO_{(Act)}$ | 0.003 | 0.003 | 0.000 | 1.00 | 1.00 |
| $OC_{(Act)}$ | 0.007 | 0.026 | 0.017 | 0.27 | 3.71 | $OC_{(Act)}$ | 0.010 | 0.019 | 0.014 | 0.53 | 1.90 |
| $CH_{2(Act)}$ | 0.003 | 0.005 | 0.004 | 0.60 | 1.67 | $CH_{2(Act)}$ | 0.005 | 0.006 | 0.005 | 0.83 | 1.20 |
| $O_{(Ph)}$ | 0.020 | 0.007 | 0.014 | 2.86 | 0.35 | $O_{(Ph)}$ | 0.026 | 0.026 | 0.026 | 1.00 | 1.00 |
| $C^1_{Ph}$ | 0.029 | 0.009 | 0.019 | 3.22 | 0.31 | $C^1_{Ph}$ | 0.041 | 0.029 | 0.035 | 1.41 | 0.71 |
| $C^4_{Ph}$ | 0.005 | 0.011 | 0.008 | 0.45 | 2.20 | $C^4_{Ph}$ | 0.014 | 0.018 | 0.016 | 0.78 | 1.29 |
| $C_{Hz}$ | 0.055 | 0.016 | 0.036 | 3.44 | 0.29 | $C_{Hz}$ | 0.072 | 0.042 | 0.057 | 1.71 | 0.58 |
| $N^1_{Hz}$ | 0.016 | 0.012 | 0.014 | 1.33 | 0.75 | $N^1_{Hz}$ | 0.044 | 0.024 | 0.034 | 1.83 | 0.55 |
| $N^2_{Hz}$ | 0.021 | 0.017 | 0.019 | 1.24 | 0.81 | $N^2_{Hz}$ | 0.020 | 0.055 | 0.038 | 0.36 | 2.75 |
| $S_{thia1}$ | 0.065 | 0.061 | 0.063 | 1.07 | 0.94 | $S_{thia1}$ | 0.076 | 0.062 | 0.069 | 1.23 | 0.82 |
| $C_{thia2}$ | 0.049 | 0.007 | 0.028 | 7.00 | 0.14 | $C_{thia2}$ | 0.044 | 0.016 | 0.030 | 2.75 | 0.36 |
| $N_{thia3}$ | 0.030 | 0.014 | 0.022 | 2.14 | 0.47 | $N_{thia3}$ | 0.039 | 0.034 | 0.037 | 1.15 | 0.87 |
| $C_{thia4}$ | 0.054 | 0.008 | 0.031 | 6.75 | 0.15 | $C_{thia4}$ | 0.039 | 0.027 | 0.033 | 1.44 | 0.69 |
| $C_{thia5}$ | 0.028 | 0.016 | 0.022 | 1.75 | 0.57 | $C_{thia5}$ | 0.028 | 0.042 | 0.035 | 0.67 | 1.50 |
| $O_{(thia4)}$ | 0.075 | 0.028 | 0.052 | 2.68 | 0.37 | $CMe_{(thia4)}$ | 0.014 | 0.011 | 0.012 | 1.27 | 0.79 |
| $CH_{(Bz)}$ | 0.074 | 0.023 | 0.049 | 3.22 | 0.31 | $CO_{Ac(thia5)}$ | 0.050 | 0.020 | 0.035 | 2.50 | 0.40 |
| $C^1Ph_{(Bz)}$ | 0.004 | 0.012 | 0.008 | 0.33 | 3.00 | $OC_{Ac(thia5)}$ | 0.075 | 0.053 | 0.064 | 1.42 | 0.71 |
| $C^4Ph_{(Bz)}$ | 0.033 | 0.021 | 0.027 | 1.57 | 0.64 | $CMe_{Ac(thia5)}$ | 0.015 | 0.009 | 0.012 | 1.67 | 0.60 |
| Cl | 0.067 | 0.052 | 0.059 | 1.29 | 0.78 | | | | | | |
| **8** | | | | | | | | | | | |
| **Atom** | $f_k^+$ | $f_k^-$ | $f_k^0$ | $s_k^+/s_k^-$ | $s_k^-/s_k^+$ | | | | | | |
| $N_{Py1}$ | 0.009 | 0.010 | 0.010 | 0.90 | 1.11 | | | | | | |
| $N_{Py2}$ | 0.005 | 0.005 | 0.005 | 1.00 | 1.00 | | | | | | |
| $C_{Py3}$ | 0.003 | 0.002 | 0.002 | 1.50 | 0.67 | | | | | | |
| $C_{Py4}$ | 0.000 | 0.000 | 0.000 | 0.00 | 0.00 | | | | | | |
| $C_{Py5}$ | 0.013 | 0.006 | 0.010 | 2.17 | 0.46 | | | | | | |
| $O_{(Py3)}$ | 0.002 | 0.004 | 0.003 | 0.50 | 2.00 | | | | | | |
| $C^1_{Ph(Py2)}$ | 0.002 | 0.002 | 0.002 | 1.00 | 1.00 | | | | | | |
| $CMe_{(Py1)}$ | 0.005 | 0.004 | 0.005 | 1.25 | 0.80 | | | | | | |
| $CMe_{(Py5)}$ | 0.004 | 0.002 | 0.003 | 2.00 | 0.50 | | | | | | |
| $NH_{(Act)}$ | 0.005 | 0.003 | 0.004 | 1.67 | 0.60 | | | | | | |
| $CO_{(Act)}$ | 0.006 | 0.002 | 0.002 | 3.00 | 0.33 | | | | | | |
| $OC_{(Act)}$ | 0.021 | 0.014 | 0.017 | 1.50 | 0.67 | | | | | | |
| $CH_{2(Act)}$ | 0.008 | 0.006 | 0.007 | 1.33 | 0.75 | | | | | | |
| $O_{(Ph)}$ | 0.029 | 0.036 | 0.032 | 0.81 | 1.24 | | | | | | |
| $C^1_{Ph}$ | 0.051 | 0.040 | 0.045 | 1.28 | 0.78 | | | | | | |
| $C^4_{Ph}$ | 0.028 | 0.020 | 0.024 | 1.40 | 0.71 | | | | | | |
| $C_{Hz}$ | 0.078 | 0.056 | 0.067 | 1.39 | 0.72 | | | | | | |
| $N^1_{Hz}$ | 0.082 | 0.031 | 0.056 | 2.65 | 0.38 | | | | | | |
| $N^2_{Hz}$ | 0.030 | 0.073 | 0.052 | 0.41 | 2.43 | | | | | | |
| $S_{thia1}$ | 0.046 | 0.083 | 0.064 | 0.55 | 1.80 | | | | | | |
| $C_{thia2}$ | 0.010 | 0.021 | 0.015 | 0.48 | 2.10 | | | | | | |
| $N_{thia3}$ | 0.035 | 0.044 | 0.040 | 0.80 | 1.26 | | | | | | |
| $C_{thia4}$ | 0.022 | 0.045 | 0.033 | 0.49 | 2.05 | | | | | | |
| $C_{thia5}$ | 0.034 | 0.064 | 0.049 | 0.53 | 1.88 | | | | | | |
| $CH_{2(thia4)}$ | 0.006 | 0.009 | 0.008 | 0.67 | 1.50 | | | | | | |
| $CO_{Est(thia4)}$ | 0.001 | 0.000 | 0.000 | 0.00 | 0.00 | | | | | | |
| $O^1C_{Est(thia4)}$ | 0.014 | 0.022 | 0.018 | 0.64 | 1.57 | | | | | | |
| $O^2C_{Est(thia4)}$ | 0.001 | 0.000 | 0.000 | 0.00 | 0.00 | | | | | | |
| $CEt_{(thia4)}$ | 0.002 | 0.003 | 0.003 | 0.67 | 1.50 | | | | | | |

the radical attack Fukui's indices ($f_k^0$) data presented different patterns but comparable to that of nucleophilic attack ($f_k^+$), e.g., compound **2** exhibited the following order $OCH_{(Ph)} > CHO_{(Ph)} > O_{(Py3)}$. While, the electrophilic attack Fukui's indices ($f_k^-$) revealed diverse patterns for the highly susceptible atoms in which the thiazole sulfur atom, $S_{thia1}$, occupied the first place in compounds **4** and **6**–**8** while the pyrazolone oxygen, $O_{(Py3)}$, in **2** and **5** was the top (Table 3).

To sidestep the Fukui's indices unreliability in some cases and detect the desirable site for nucleophilic and electrophilic attack, the local relative electrophilicity and nucleophilicity descriptors, $s_k^-/s_k^+$ and $s_k^+/s_k^-$, respectively, were calculated

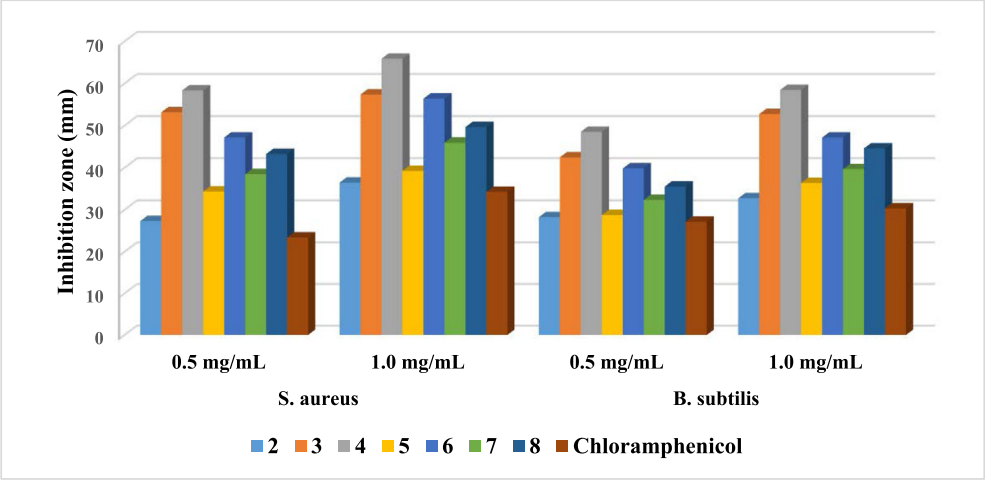


**Fig. 6** Antibacterial activity of the tested compounds against Gram's positive bacteria.

(Roy et al., 1998b, Roy et al., 1998a, Roy et al., 1999), where $\delta$ is global softness, $s_k^+ = f_k^+ \times \delta$ and $s_k^- = f_k^- \times \delta$. The relative nucleophilicity descriptors data, $s_k^+/s_k^-$, offered diverse susceptible atoms patterns, e.g., the derivative **2** has $O_{(Ph)}$ > $CHO_{(Ph)}$ > $OCH_{(Ph)}$ order while **3** presented $C_{Py5}$ > $N_{Hz}^{1}$ > $CS_{Hz}$. On the other hand, the relative electrophilicity descriptors, $s_k^-/s_k^+$, data revealed dissimilar patterns in which the pyrazolone carbon, $C_{Py3}$, occupied the first place in compounds **2**, **6** and **7** while acetamide carbonyl carbon, $CO_{(Act)}$, in **3**, thiazole carbon, $C_{thia2}$, in **4**, pyrazolone oxygen, $O_{(Py3)}$, in **5** and hydrazinic nitrogen, $N_{Hz}^{2}$, in **8** were the most susceptible sites (Table 3).

### *3.3. Antibacterial and antifungal activity*

Antibacterial efficiency for the prepared antipyrine-thiazole hybrids, at two different concentrations (0.5 and 1.0 mg/mL), was screened against two representative Gram's positive strains, *S. aureus* (ATCC 25923) and *B. subtilis* (ATCC 6635), and Gram's negative strains, *S. typhimurium* (ATCC 14028) and *E. coli* (ATCC 25922) through the spectrum of disc-agar technique (Azoro, 2002), where Chloramphenicol and Cephalothin were exploited as drug references, respectively.

Generally, the data, shown in Fig. 6, indicated that the derivatives containing thiazole moiety possess a significant bactericidal activity, especially against *S. aureus* more than *B. subtilis* as Gram's + ve bacteria (Al-Anazi et al., 2019; Gondru et al., 2021). So, the antipyrinyl derivative **2** displayed the expected lowest activity (27.33 ± 0.65 and 36.46 ± 0.16 mg/mL) rather than the rest of hybrids due to it haven't contained thiazole ring in its structure. The thiosemicarbazide branch **3** revealed a significant effectiveness (53.15 ± 0.39 and 57.38 ± 0.21 mg/mL) against Gram's + ve bacteria (Siwek et al., 2011). On the other hand, Antipyrine-thiazole hybrid **4**, which contains chlorophenyl moiety, displayed eminent antibacterial activity (58.35 ± 0.28 and 65.88 ± 0.52 mg/mL). This may be attributed to the presence of chlorophenyl-thiazole moiety as an electron donating group (Mohammad et al., 2017). Meanwhile, the antipyrine-thiazole derivative **6**, that has benzylidine conjugate, displayed a respectable antibacterial activity (47.16 ± 0.12 and 56.43 ± 0.07 mg/mL) (Sharma et al., 2013), which is referred to the conjugation existed in benzylidine-thiazole moiety (Bharti et al., 2010). Moreover, the synthesized of ester substituted antipyrine-thiazole **8**, demonstrated a higher activity (43.25 ± 0.51 and 49.67 ± 0.23 mg/mL) than the acetyl thiazole compound **7** (38.47 ± 0.02 and 45.93 ± 0.18 mg/mL) while the antipyrine-thiazole **5** showed a lower reactivity (34.37 ± 0.29 and 39.26 ± 0.08 mg/mL) which may due to that it contains thiazolin-4-one moiety (Gaballah et al., 2019).

Meanwhile, the synthesized antipyrine-thiazole hybrids displayed a promising efficacy against Gram's negative bacteria, *S. typhimurium* and *E. coli*, in comparison to Cephalothin as a reference drug (Fig. 7). The difference in the antibacterial activity is due to the mechanism of action resulted from the thiazolyl moiety (Kriek et al., 2007).

The antifungal activity of the antipyrinyl-thiazole hybrids was screened against *Candida albicans* and *Aspergillus fumigatus*, utilizing Cycloheximide as a reference drug at two different concentrations, 0.5 and 1.0 mg/mL, respectively. All examined compounds exhibited high inhibition effect toward *C. albicans* and this is agreed with recent literature (de Sá et al., 2021). Among the antipyrinyl-thiazole derivatives, compounds **3**, **7** and **8** displayed strong activity against *C. albicans* while all the synthesized hybrids exhibited eminent activity against *A. fumigatus* (Fig. 8). Rendering to antifungal results, it was clear that the presence of antipyrinyl-thiazole moieties presented a higher efficacy toward fungal strains.

Furthermore, the minimum inhibition concentration (MIC) values of the antipyrinyl-thiazole derivatives were determined against the studied bacterial strains and *C. albicans*. In accordance, the antipyrinyl-thiazole hybrids showed higher activity against Gram's positive bacteria where compounds **3**,**4** and **6** revealed eminent influences toward *S. aureus* with minimal concentrations, MIC = 28–35 μg/mL, and toward *B. subtilis*, MIC = 44–51 μg/mL. However, hybrid **4** displayed respectable activity against Gram's negative *S. typhimurium* and *E. coli* where its MIC was 34 and 111 μg/mL, respectively, matched to Cephalothin as a reference. Likewise, derivatives **7** and **8** demonstrated good antifungal efficacy toward *C. albicans* (MIC = 168 and 172 μg/mL) in contrast to Cycloheximide grade (Table 4).

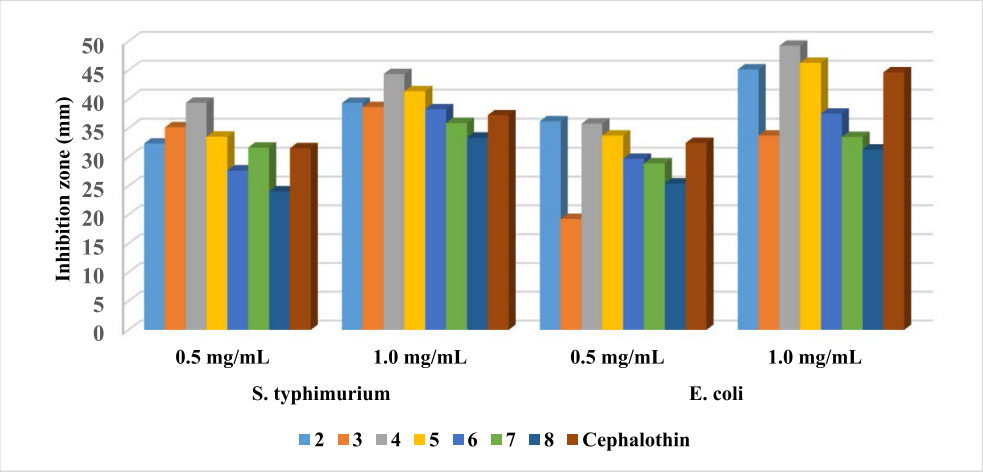


**Fig. 7** Antibacterial activity of the tested compounds against Gram's negative bacteria.

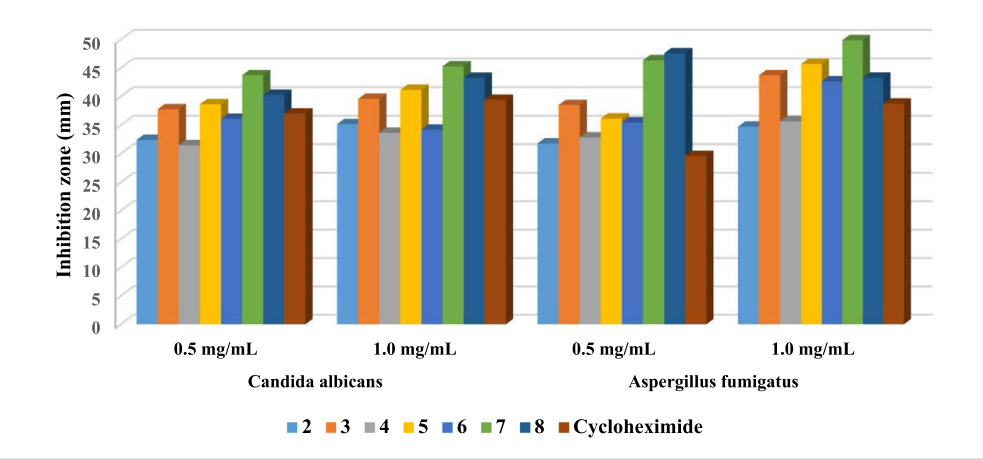


**Fig. 8** Antifungal activity of the investigated compounds against two different fungal strains.

**Table 4** Biological activities of the synthesized compounds in minimal inhibition concentrations (MIC, μg/mL).

| Compound | Gram's positive bacteria | | Gram's negative bacteria | | Fungi |
|---|---|---|---|---|---|
| | *S. aureus* | *B. subtilis* | *S. typhimurium* | *E. coli* | *C. albicans* |
| **2** | 61 | 73 | 61 | 166 | 237 |
| **3** | 32 | 51 | 69 | 158 | 219 |
| **4** | 28 | 44 | 34 | 111 | 233 |
| **5** | 58 | 77 | 41 | 148 | 224 |
| **6** | 35 | 48 | 44 | 154 | 245 |
| **7** | 47 | 62 | 57 | 152 | 168 |
| **8** | 49 | 56 | 49 | 168 | 172 |
| Chloramphenicol | 143 | 152 | – | – | – |
| Cephalothin | – | – | 135 | 229 | – |
| Cycloheximide | – | – | – | – | 254 |

**Notes**: Chloramphenicol and Cephalothin as a positive control for of Gram + ve and Gram-ve bacteria; Cycloheximide in the case of fungi "*C. albicans* (ATCC 10231) and *A. fumigatus*".

**Table 5** The molecular docking data of the synthesized derivatives.

| Code | S (Energy score) (Kcal/mol) | Rmsd (Refine unit) | Interaction with ligand | Types of Interactions | Distance (Å) |
|---|---|---|---|---|---|
| **2** | −5.8523 | 1.2123 | O-atom of amide group with Lys 119 | H-acceptor | 2.90 |
| | | | O-atom of aldhyde group with Gln 124 | H-acceptor | 3.15 |
| **3** | −7.4821 | 1.3934 | N1- atom of thiourea with Glu 183 | H-donor | 2.81 |
| | | | N2– atom of thiourea with Glu 183 | H-donor | 2.93 |
| | | | N3 of thiosemicarbazone with Arg 186 | H-acceptor | 3.24 |
| | | | S-atom of thiosemicarbazone with Arg 186 | H-acceptor | 4.25 |
| | | | O-atom of amide group with Ser 116 | H-acceptor | 2.95 |
| | | | O-atom of pyrazolone ring with Ser 262 | H-acceptor | 3.02 |
| **4** | −7.6280 | 2.8086 | N-atom of amide group with Ser 75 | H-donor | 3.18 |
| | | | S-atom of thiazole ring with Asp 264 | H-donor | 4.37 |
| **5** | −6.9005 | 1.6405 | S-atom of thiazolidinone ring with Asp 264 | H-donor | 3.42 |
| | | | N-atom of thiazolidinone ring with Arg 186 | H-acceptor | 3.30 |
| | | | N-atom of hydrazo group with Arg 186 | H-acceptor | 3.31 |
| **6** | −7.4437 | 1.6878 | O- atom of pyrazolone ring with Ser 264 | H-acceptor | 3.05 |
| | | | O-atom of amide group with Ser 116 | H-acceptor | 3.10 |
| **7** | −7.3314 | 1.6523 | S-atom of thiazole ring with Asp 264 | H-donor | 3.16 |
| | | | N-atom of thiazole ring with Arg 186 | H-acceptor | 3.12 |
| | | | N-atom of hydrazo group with Asp 264 | H-donor | 2.92 |
| **8** | −7.3471 | 1.4377 | N- atom of amide group with Glu 183 | H-donor | 3.00 |
| | | | C-atom of Methylene ester with Glu 183 | H-donor | 3.25 |
| | | | O-atom of amide group with Arg 186 | H-acceptor | 2.95 |
| | | | S-atom of thiazole ring with Ser 75 | H-donor | 3.21 |
| | | | S-atom of thiazole ring with Ser 139 | H-donor | 4.22 |
| | | | Thiazole ring with Ser 262 | π-π | 4.61 |
| **Chloramphenicol** | −6.3989 | 1.2989 | O-atom of hydroxyl group with Ser 262 | H-donor | 2.97 |
| | | | O-atom of nitro ring with Arg 300 | H-acceptor | 3.45 |

### *3.4. Molecular docking studies*

The molecular docking process was applied on the antipyrinyl-thiazole hybrids toward distinct binding sites of *S. aureus* "Homo sapiens"(pdb: 3HUN) protein after removal the water and the heteroatoms. Table 5 data indicated that compound **2** was offered weak bind score, S = -5.8523 kcal/mol, with two H-acceptor bonds between O-atoms of both of amide and aldehyde groups and Lys 119 and Gln 124 over (2.90 and 3.15 Å), respectively (Fig. S1). Whereas, derivative **3** showed acceptable binding score, S = -5.8523 kcal/mol, over forming six interesting H-bonds between Glu 183 with $N^1$, $N^2$ and $N^4$ atoms of thiosemicarbazide moiety with Arg 186 (2.81, 2.93 and 3.24 Å, respectively), S-atom of thiosemicarbazone with Arg 186 (4.25 Å), O-atom of amide group with Ser 116 (2.95 Å), and O-atom of pyrazolone ring with Ser 262 (3.02 Å) (Fig. 9).

Furthermore, the compound **4** exhibited the highest binding score, S = -7.628 kcal/mol, through establishing two remarkable H-donor bonds between N-atom of the amide with amino acid Ser 175 and S-atom of thiazole ring with Asp 264 over (3.18 and 4.37 Å, respectively) (Fig. 10).

Moreover, hybrid **5** demonstrated the lowest binding score, S = -6.9005 kcal/mol, over three intermolecular H-bonds between S-atom of thiazolidinone ring with Asp 264 (3.42 Å), N-atom of thiazolidinone ring with Arg 186 (3.30 Å) and N-atom of hydrazo group with Arg 186 (3.31 Å) (Fig. S2). However, derivative **6** presented higher binding score, S = -7.4437 kcal/mol, through two H-bonds between O-atom of pyrazolone ring with Ser 264 (3.05 Å) and O-atom of amide group with Ser 116 (3.10 Å), while hybrid **7** displayed comparable binding score, S = -7.3314 kc al/mol, by three H-bonds between S-atom of thiazole ring with Ser 264 (3.16 Å), N-atom of thiazole ring with Arg 186 (3.12 Å) and N-atom of hydrazo group with Asp 264 (2.92 Å) (Figs. S3 and S4). Furthermore, hybrid **8** was exhibited binding score S = -7.3314 kcal/mol *via* two different types of interactions, five H-bonds and one π-π interaction. The five H-bonds was arisen through two H-donor bonds between Glu 183 with both of N-atom of amide group and C-atom of Methylene ester (3.00 and 3.25 Å), H-acceptor bond between O-atom of amide group with Arg 186(2.95 Å), two H-donor bonds between S-atom of thiazole ring with both of Ser 75 and Ser 139 (3.21 and 4.22 Å), respectively. Then π-π interaction was presented between the thiazole ring and Ser 262 through intermolecular distance (4.61 Å) (Fig. S5). In addition, Chloramphenicol drug was screened against (pdb: 3HUN) protein and offered binding score −6.3989 kcal/mol through two H-donor bonds between O-atom of hydroxyl group with Ser 262, O-atom of nitro group with Arg 300 over intermolecular distance (2.97 and 3.45 Å), respectively (Fig. S6).

On the other hand, the new antipyrine-thiazole hybrids was were examined toward diverse binding sites of *E.coli* "Homo sapiens" (PDB: 2EXB) protein after removal both of water and heteroatoms. Table 6 data designated that hybrid **2** was presented the lowest bind score, S = -5.6971 kcal/mol, through π-H interaction between Pyrazolone ring with Ala 245 (3.88 Å), and two H-acceptor bonds between O-atoms of both of amide and aldehyde groups and Ala 245and Val 221over (3.09 and 3.42 Å), respectively ((Fig. S7). However,

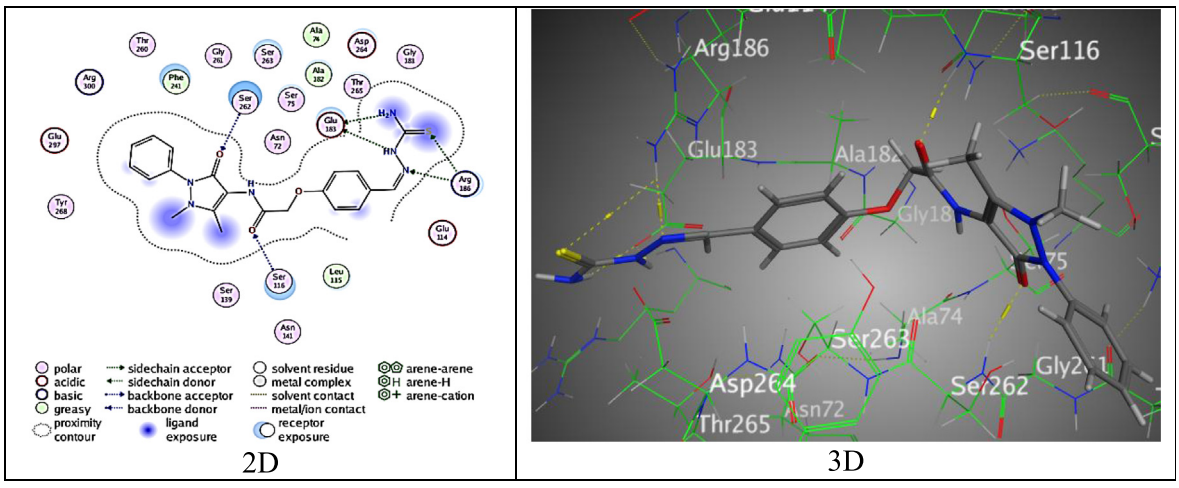


**Fig. 9** The binding mode of **3** with 3HUN.

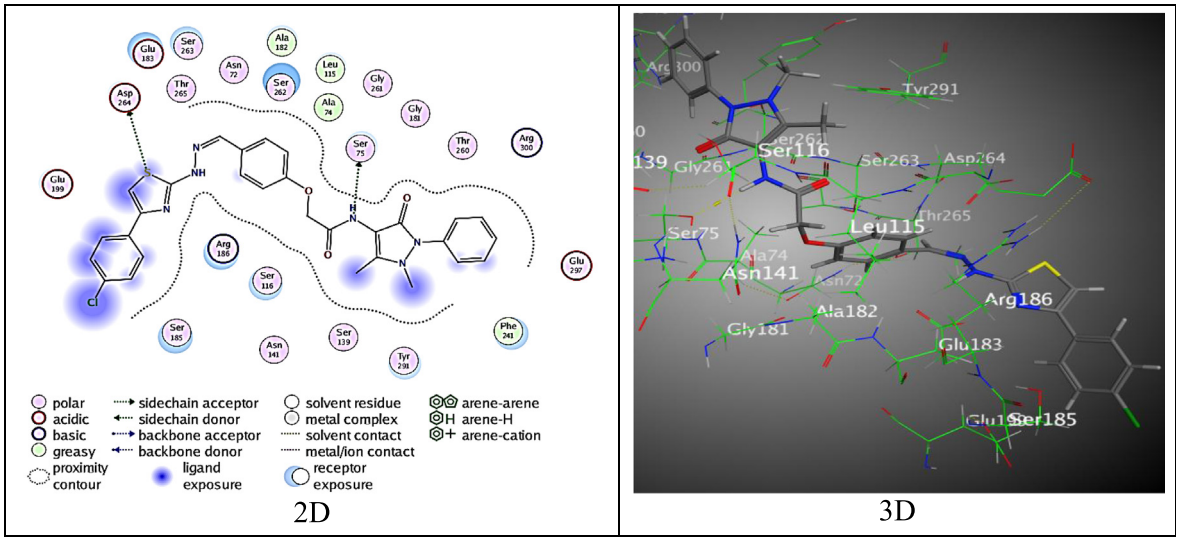


**Fig. 10** The binding mode of **4** with 3HUN.

hybrid **3** exhibited adequate binding score, S = −5.8879 kcal/-mol, two interesting H-bonds between N- atom of amide group with Val 221and S-atom of thiosemicarbazone with Ala 245 in addition to Pyrazolone ring with Val 221 through (3.15, 3.43 and 4.29 Å, respectively ((Fig. S8).

Likewise, the hybrid **4** exhibited good binding score, S = -7.0092 kcal/mol, over establishing three diverse H- bonds between Nitrogen and Oxygen atoms of the amide moiety with PDB: 2EXB amino acid through Gln 158and Ala 245, O-atom of Pyrazolone ring with Cys 159, π-H interaction between Pyrazolone ring and Val 222 over (2.85, 3.01, 2.96 and 3.95 Å, respectively) (Fig. 11).

Meanwhile, hybrids **5** and **6** were displayed respectable bind scores S = −6.3964 and-6.8384 kcal/mol, two types of H-donor and H-acceptor came from Oxgen and Nitrogen atoms of amide group with both of Ala 245 and Gln 158 amino-acids (Figs. S9 and S10).

Hybrid 7 presented four diverse interactions between O-atom of amide group with Val 221, Gln 158 with both of S-atom of thiazole ring and N-atom of hydrazo group, and Pyrazolone ring with Val 222, through proper bind score, S = -6.3406 kcal/mol (Fig. S11).

Moreover, hybrid **8** exhibited an eminent bind score, S = -7.4200 kcal/mol through two H-bonds between amide group with Gln 158 and Ala 245 came from Nitrogen and Oxygyen atoms, H-acceptor between O-atom of Pyrazolone ring with Cys 159, and Pyrazolone ring with Ala 245 through π-H interaction (Fig. 12).

Furthermore, Cephalothin reference was applied against (pdb: 2EXB) protein and presented binding score −6.4299 kcal/mol over three H-donor bonds, two H-bonds between O-atoms of both of amide and aldehyde groups and Ala 245and Val 221over (2.81 and 2.91 Å), and the third was arised between O-atom of hydroxyl group with Asn 145 (Fig. S12).

Lastly, the docking results presented the following: 1) Hybrids **3, 4,** and **6** were revealed good binding scores −7.4821, −7.6280, and −7.4437 kcal/mol against the amino-

**Table 6** The molecular docking data of the synthesized derivatives.

| Code | S (Energy score) (Kcal/mol) | Rmsd (Refine unit) | Interaction with ligand | Types of Interactions | Distance (Å) |
|---|---|---|---|---|---|
| **2** | −5.6971 | 1.4235 | O-atom of amide group with Ala 245 | H-acceptor | 3.09 |
| | | | O-atom of aldhyde group with Val 221 | H-acceptor | 3.42 |
| | | | Pyrazolone ring with Ala 245 | π-H | 3.88 |
| **3** | −5.8879 | 1.0429 | N- atom of amide group with Val 221 | H-donor | 3.15 |
| | | | S-atom of thiosemicarbazone with Ala 245 | H-acceptor | 3.43 |
| | | | Pyrazolone ring with Val 221 | π-H | 4.29 |
| **4** | −7.0092 | 1.2816 | N-atom of amide group with Gln 158 | H-donor | 2.85 |
| | | | O-atom of amide group with Ala 245 | H-acceptor | 3.01 |
| | | | O-atom of Pyrazolone ring with Cys 159 | H-acceptor | 2.96 |
| | | | Pyrazolone ring with Ala 245 | π-H | 3.95 |
| **5** | −6.3964 | 0.9840 | N-atom of amide group with Gln 158 | H-donor | 3.09 |
| | | | O-atom of amide group with Ala 245 | H-acceptor | 3.07 |
| **6** | −6.8384 | 1.2619 | O-atom of amide group with Ala 245 | H-acceptor | 2.96 |
| | | | N-atom of amide group with Gln 158 | H-donor | 3.23 |
| **7** | −6.3406 | 1.5805 | O-atom of amide group with Val 221 | H-acceptor | 2.98 |
| | | | S-atom of thiazole ring with Gln 158 | H-donor | 3.12 |
| | | | N-atom of hydrazo group with Gln 158 | H-donor | 3.13 |
| | | | Pyrazolone ring with Val 222 | π-H | 4.01 |
| **8** | −7.4200 | 1.6759 | N- atom of amide group with Gln 158 | H-donor | 2.82 |
| | | | O-atom of amide group with Ala 245 | H-acceptor | 2.96 |
| | | | O-atom of Pyrazolone ring with Cys 159 | H-acceptor | 3.01 |
| | | | Pyrazolone ring with Ala 245 | π-H | 3.74 |
| **Cephalothin** | −6.4299 | 0.9437 | N-atom of amide group with Gln 158 | H-donor | 2.81 |
| | | | O-atom of amide group with Ala 245 | H-acceptor | 2.91 |
| | | | O-atom of hydroxyl group with Asn 145 | H-donor | 3.10 |

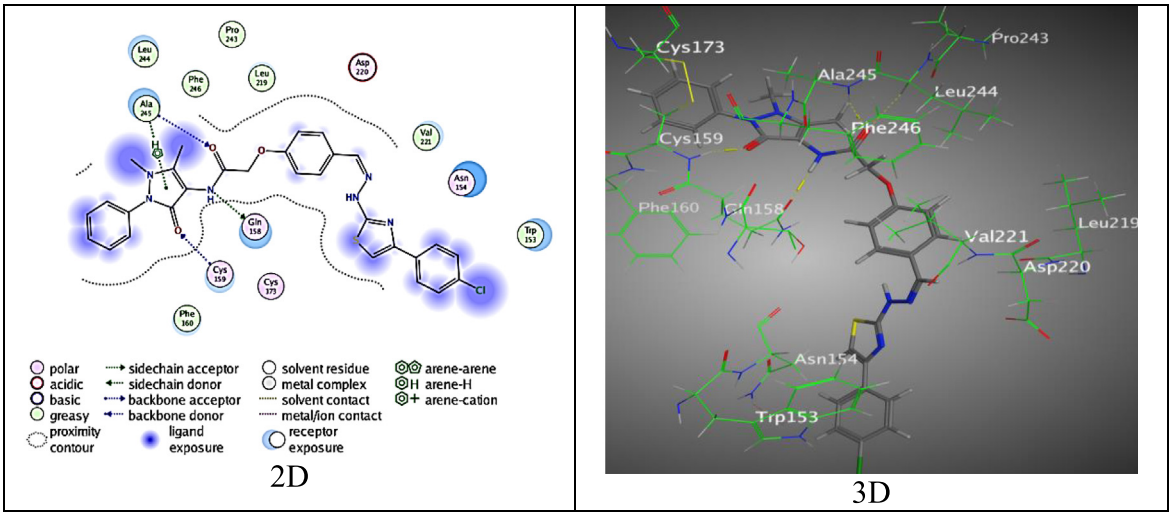


**Fig. 11** The binding mode of **4** with (PDB ID: 2EXB).

acids of 3HUN while hybrids **4** and **8** were discovered respectable binding scores −7.0092 and −7.4200 kcal/mol alongside the amino-acids of 2EXB. 2) The two- and three-dimensional pictures of utmost hybrids presented good association between the O and N atoms of the amide group beside N and S atoms of the on the thiazole ring through an intramolecular hydrogen bond with dissimilar amino-acids for both of 3HUN and 2EXB. 3) The substituents on pocket size of 3HUN and 2EXB could be defined as fissures that were controlled by stereotypically scarce polar residue explicit binding sites (Asp 264, Arg 84, Ser 262, Glu 183 and Cys139) for 3HUN and (Ala 245, Val 221, Gln 158) as detailed in the two-dimensional images, and presented appropriate cavity of the antipyrinyl-thiazole hybrids.

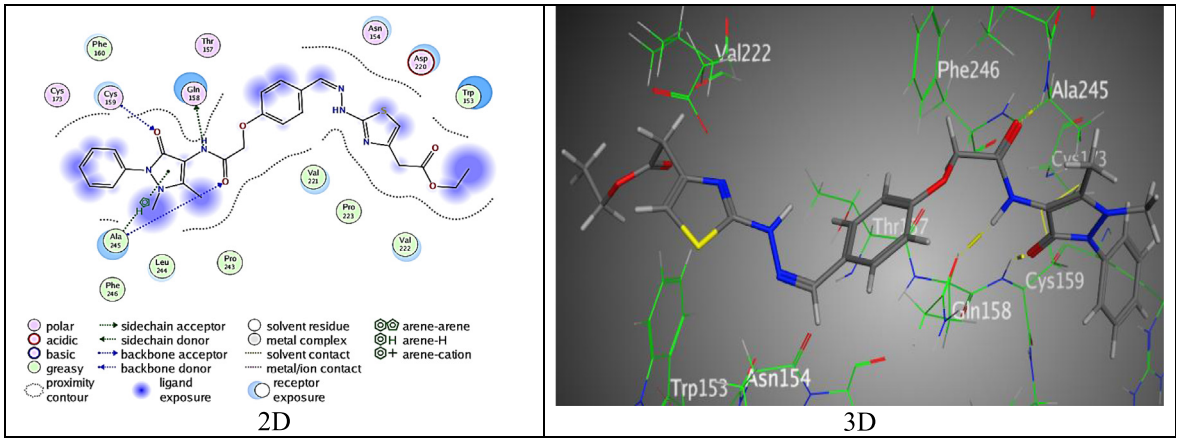


**Fig. 12** The binding mode of **8** with (PDB ID: 2EXB).

## 4. Conclusion

A series of new antipyrine-thiazole hybrids having phenoxyacetamide moiety as a link bridge was synthesized. The quantum chemical calculations at DFT/B3LYP level were used to determine the HOMO-LUMO energies and Fukui's indices toward nucleophilic, electrophilic and radical attacks. The investigated compounds were arranged due to HOMO-LUMO energy gap as following **6** < **5** < **7** < **3** < **2** < **4** < **8**. Antibacterial and antifungal activities for the synthesized antipyrine-thiazole hybrids were demonstrated remarkable activity against *S. aureus* than *B. subtilis* (gram + ve strain), in relationship to the outcomes of chloramphenicol. Where, hybrids **3**, **4**, **6** and **8** recorded a significant MIC values (MIC = 28–35 μg/mL) toward *S. aureus*, and (MIC = 44–51 μg/mL) toward *B. subtilis*. However, hybrid **4** displayed respectable activity against *S. typhimurium* and *E. coli* MIC = 34 and 111 μg/mL, respectively, matched to Cephalothin as reference. Likewise, hybrids **7** and **8** were demonstrated good antifungal efficacy toward *C. albicans* (MIC = 168 and 172 μg/mL) in contrast to Cycloheximide grade. Molecular docking studies was pragmatic to stimulate the reactivity of the synthesized hybrids against different binding sites of *Staphylococcus aureus* "Homo sapiens" (PDB: 3HUN) protein and *E.coli* "Homo sapiens" (PDB: 2EXB) protein. The theoretical and practical antibacterial and antifungal activities results in this work designated a proper agreement.

## Declaration of Competing Interest

The authors declare that they have no known competing financial interests or personal relationships that could have appeared to influence the work reported in this paper.

## Acknowledgements

The financial support by the Deanship of Scientific Research (GRP-53-43), King Khalid University Saudi Arabia is gratefully acknowledged.

## Appendix A. Supplementary data

Supplementary data to this article can be found online at https://doi.org/10.1016/j.arabjc.2022.103898.

## References

Al-Anazi, K.M., Mahmoud, A.H., Abulfarah, M., Allam, A.A., Fouda, M.M., Gaffer, H.E., 2019. 2-Amino-5-arylazothiazole-Based Derivatives. In Vitro Cytotoxicity, Antioxidant Properties, and Bleomycin-Dependent DNA Damage. ChemistrySelect 4, 5570–5576.

Azoro, C., 2002. Antibacterial activity of Crude Extract of Azudirachita indica on Salmonella typhi. World J. Biotechnol. 3, 347–351.

Badorc, A., Bordes, M.F., De Cointet, P., Savi, P., Bernat, A., Lale, A., Petitou, M., Maffrand, J.P., Herbert, J.M., 1997. New orally active non-peptide fibrinogen receptor (GpIIb-IIIa) antagonists: identification of ethyl 3-[N-[4-[4-[amino [(ethoxycarbonyl) imino] methyl] phenyl]-1, 3-thiazol-2-yl]-N-[1-[(ethoxycarbonyl) methyl] piperid-4-yl] amino] propionate (SR 121787) as a potent and long-acting antithrombotic agent. J. Med. Chem. 40, 3393–3401.

Bagheri, M., Shekarchi, M., Jorjani, M., Ghahremani, M.H., Vosooghi, M., Shafiee, A., 2004. Synthesis and Antihypertensive Activity of 1-(2-Thiazolyl)-3, 5-disubstituted-2-Pyrazolines. *Archiv der Pharmazie*. Int. J. Pharm. Med. Chem. 337, 25–34.

Bakir, M., 2018. X-ray crystallographic, spectroscopic and electrochemical properties of a bi-stable di-2-thienyl ketone 2, 4-dinitrophenyl hydrazone (dtkdnph). J. Mole. Struct. 1173, 942–950.

Bakir, M., Hassan, I., Johnson, T., Brown, O., Green, O., Gyles, C., Coley, M.D., 2004. X-ray crystallographic, electrochemical and spectroscopic properties of 2-pyridinio 2-pyridyl ketone phenyl hydrazone chloride hydrate. J. Mole. Struct. 688, 213–222.

Bakir, M., Lawrence, M.A., Nelson, P.N., Conry, R.R., 2016. Spectroscopic and electrochemical properties of di-2-thienyl ketone thiosemicarbazone (dtktsc): electrochemical reactions with electrophiles (H + and CO2). Electrochim. Acta 212, 1010–1020.

Bakir, M., Lawrence, M.W., Yamin, M.B., 2020. Novel κ2-Nim, S-and κ4-C, Nim,(μ-S),(μ-S)-coordination of di-2-thienyl ketone thiosemicarbazone (dtktsc). Hydrogen evolution and catalytic properties of palladacyclic [Pd (κ4-C, Nim,(μ-S),(μ-S)-dtktsc-2H)] 4. Inorg. Chim. Acta 507, 119592.

Becke, A.D., 1993. Density-functional thermochemistry. III. The role of exact exchange. J. Chem. Phys. 98, 5648–5652.

Benassi, R., Folli, U., Iarossi, D., Schenetti, L., Taddei, F., Musatti, A., Nardelli, M., 1989. Conformational analysis of organic carbonyl compounds. Part 11. Conformational properties of difuryl, dithienyl, and furyl thienyl ketones studied by X-ray crystallography, NMR lanthanide-induced shifts and ab-initio MO calculations. J. Chem. Soc. Perkin Transactions 2, 1741–1751.

Bhagyasree, J.B., Varghese, H.T., Panicker, C.Y., Samuel, J., Van Alsenoy, C., Bolelli, K., Yildiz, I., Aki, E., 2013. Vibrational spectroscopic (FT-IR, FT-Raman, (1)H NMR and UV) investigations and computational study of 5-nitro-2-(4-nitrobenzyl) benzoxazole. Spectrochim Acta A Mol Biomol. Spectrosc. 102, 99–113.

Bharti, S., Nath, G., Tilak, R., Singh, S., 2010. Synthesis, antibacterial and anti-fungal activities of some novel Schiff bases containing 2, 4-disubstituted thiazole ring. Eur. J. Med. Chem. 45, 651–660.

Biernasiuk, A., Kawczyńska, M., Berecka-Rycerz, A., Rosada, B., Gumieniczek, A., Malm, A., Dzitko, K., Łączkowski, K.Z., 2019. Synthesis, antimicrobial activity, and determination of the lipophilicity of ((cyclohex-3-enylmethylene) hydrazinyl) thiazole derivatives. Med. Chem. Res. 28, 2023–2036.

Biovia, D.S., 2017. Materials Studio. Dassault Systèmes, San Diego.

Bouchoucha, A., Zaater, S., Bouacida, S., Merazig, H., Djabbar, S., 2018. Synthesis and characterization of new complexes of nickel (II), palladium (II) and platinum(II) with derived sulfonamide ligand: Structure, DFT study, antibacterial and cytotoxicity activities. J. Mole. Struct. 1161, 345–355.

Bulat, F.A., Chamorro, E., Fuentealba, P., Toro-Labbe, A., 2004. Condensation of frontier molecular orbital Fukui functions. J. Phys. Chem. A 108, 342–349.

De Sá, N.P., De Barros, P.P., Junqueira, J.C., Valerio, A.D., Lino, C. I., De Oliveira, R.B., Rosa, C.A., Johann, S., 2021. Antivirulence activity and in vivo efficacy of a thiazole derivative against candidiasis. J. Med. Mycol. 31, 101134.

Deb, P.K., Kaur, R., Chandrasekaran, B., Bala, M., Gill, D., Kaki, V. R., Akkinepalli, R.R., Mailavaram, R., 2014. Synthesis, anti-inflammatory evaluation, and docking studies of some new thiazole derivatives. Med. Chem. Res. 23, 2780–2792.

Delley, B., 2006. Ground-state enthalpies: evaluation of electronic structure approaches with emphasis on the density functional method. J. Phys. Chem. A 110, 13632–13639.

Dhillon, S., 2016. Dabrafenib plus Trametinib: A review in advanced melanoma with a BRAF V600 mutation. Targeted oncol. 11, 417–428.

Distefano, G., De Palo, M., Dal Colle, M., Guerra, M., 1998. Ab initio determination of the geometric structure of oligo-2-thienyl ketones. J. Mole. Struct. THEOCHEM 455, 131–140.

El Adnani, Z., Mcharfi, M., Sfaira, M., Benzakour, M., Benjelloun, A., Touhami, M.E., 2013. DFT theoretical study of 7-R-3methylquinoxalin-2 (1H)-thiones (RH; $CH_3$; Cl) as corrosion inhibitors in hydrochloric acid. Corr. Sci. 68, 223–230.

El Sayed, M.T., El-Sharief, M.A.S., Zarie, E.S., Morsy, N.M., Elsheakh, A.R., Voronkov, A., Berishvili, V., Hassan, G.S., 2018. Design, synthesis, anti-inflammatory activity and molecular docking of potential novel antipyrine and pyrazolone analogs as cyclooxygenase enzyme (COX) inhibitors. Bioorg. Med. Chem. Lett. 28, 952–957.

Frisch, M., Trucks, G., Schlegel, H., Scuseria, G., Robb, M., Cheeseman, J., Scalmani, G., Barone, V., Mennucci, B. Petersson, G. 2009. Gaussian 09, Revision A. 1. Wallingford, CT, USA: Gaussian.

Gaballah, S.T., Khalil, A.M., Rabie, S.T., 2019. Thiazole derivatives-functionalized polyvinyl chloride nanocomposites with photostability and antimicrobial properties. J. Vinyl Additive Technol. 25, E137–E146.

Gondru, R., Kanugala, S., Raj, S., Kumar, C.G., Pasupuleti, M., Banothu, J., Bavantula, R., 2021. 1, 2, 3-triazole-thiazole hybrids: Synthesis, in vitro antimicrobial activity and antibiofilm studies. Bioorg. Med. Chem. Lett. 33, 127746.

Ibáñez, L., VIDAL, X., Ballarín, E. LAPORTE, J.R. 2005. Population-based drug-induced agranulocytosis. Arch. int. Med. 165, 869-874.

Jaen, J.C., Wise, L.D., Caprathe, B.W., Tecle, H., Bergmeier, S., Humblet, C.C., Heffner, T.G., Meltzer, L.T., Pugsley, T.A., 1990. 4-(1, 2, 5, 6-Tetrahydro-1-alkyl-3-pyridinyl)-2-thiazolamines: a novel class of compounds with central dopamine agonist properties. J. Med. Chem. 33, 311–317.

Jaiswal, V., Rastogi, R.B., Kumar, R., 2014. Tribological studies of some SAPS-free Schiff bases derived from 4-aminoantipyrine and aromatic aldehydes and their synergistic interaction with borate ester. J. Mater. Chem. A 2, 10424–10434.

Kriek, M., Martins, F., Leonardi, R., Fairhurst, S.A., Lowe, D.J., Roach, P.L., 2007. Thiazole synthase from Escherichia coli: an investigation of the substrates and purified proteins required for activity in vitro. J. Biol. Chem. 282, 17413–17423.

Lee, C., Yang, W., Parr, R.G., 1988. Development of the Colle-Salvetti correlation-energy formula into a functional of the electron density. Phys. Rev. B 37, 785–789.

Lombardo, L.J., Lee, F.Y., Chen, P., Norris, D., Barrish, J.C., Behnia, K., Castaneda, S., Cornelius, L.A., Das, J., Doweyko, A.M., 2004. Discovery of N-(2-chloro-6-methyl-phenyl)-2-(6-(4-(2-hydroxyethyl)-piperazin-1-yl)-2-methylpyrimidin-4-ylamino) thiazole-5-carboxamide (BMS-354825), a dual Src/Abl kinase inhibitor with potent antitumor activity in preclinical assays. J. Med. Chem. 47, 6658–6661.

Mahle, F., Da Rosa Guimarães, T., Meira, A.V., Correa, R., Cruz, R. C.B., Cruz, A.B., Nunes, R.J., Cechinel-Filho, V.D., Campos-Buzzi, F., 2010. Synthesis and biological evaluation of N-antipyrine-4-substituted amino-3-chloromaleimide derivatives. Eur. J. Med. Chem. 45, 4761–4768.

Makhlouf, M.M., Radwan, A.S., Ghazal, B., 2018. Experimental and DFT insights into molecular structure and optical properties of new chalcones as promising photosensitizers towards solar cell applications. Appl. Surf. Sci. 452, 337–351.

Messali, M., Larouj, M., Lgaz, H., Rezki, N., Al-Blewi, F., Aouad, M., Chaouiki, A., Salghi, R., Chung, I.M., 2018. A new schiff base derivative as an effective corrosion inhibitor for mild steel in acidic media: Experimental and computer simulations studies. J. Mole. Struct. 1168, 39–48.

Mi, H., Xiao, G., Chen, X., 2015. Theoretical evaluation of corrosion inhibition performance of three antipyrine compounds. Comput. Theor. Chem. 1072, 7–14.

Mohammad, H., Younis, W., Chen, L., Peters, C.E., Pogliano, J., Pogliano, K., Cooper, B., Zhang, J., Mayhoub, A., Oldfield, E., 2017. Phenylthiazole antibacterial agents targeting cell wall synthesis exhibit potent activity in vitro and in vivo against vancomycin-resistant Enterococci. J. Med. Chem. 60, 2425–2438.

Olasunkanmi, L.O., Obot, I.B., Ebenso, E.E., 2016. Adsorption and corrosion inhibition properties of N-{n-[1-R-5-(quinoxalin-6-yl)-4, 5-dihydropyrazol-3-yl] phenyl} methanesulfonamides on mild steel in 1 M HCl: experimental and theoretical studies. RSC Adv. 6, 86782–86797.

Perdew, J.P., Wang, Y., 1992. Pair-distribution function and its coupling-constant average for the spin-polarized electron gas. Phys. Rev. B 46, 12947–12954.

Rauf, A., Kashif, M.K., Saeed, B.A., Al-Masoudi, N.A., Hameed, S., 2019. Synthesis, anti-HIV activity, molecular modeling study and QSAR of new designed 2-(2-arylidenehydrazinyl)-4-arylthiazoles. J. Mole. Struct. 1198, 126866.

Remes, C., Paun, A., Zarafu, I., Tudose, M., Caproiu, M., Ionita, G., Bleotu, C., Matei, L., Ionita, P., 2012. Chemical and biological evaluation of some new antipyrine derivatives with particular properties. Bioorg. Chem. 41, 6–12.

Roy, R., De Proft, F.D., Geerlings, P., 1998a. Site of protonation in aniline and substituted anilines in the gas phase: a study via the local hard and soft acids and bases concept. J. Phys. Chem. A 102, 7035–7040.

Roy, R., Krishnamurti, S., Geerlings, P., Pal, S., 1998b. Local softness and hardness based reactivity descriptors for predicting intra-and intermolecular reactivity sequences: carbonyl compounds. J. Phys. Chem. A 102, 3746–3755.

Roy, R.K., Pal, S., Hirao, K., 1999. On non-negativity of Fukui function indices. J. Phys. Chem. 110, 8236–8245.

Rudolph, J., Theis, H., Hanke, R., Endermann, R., Johannsen, L., Geschke, F.U., 2001. seco-Cyclothialidines: new concise synthesis, inhibitory activity toward bacterial and human DNA topoisomerases, and antibacterial properties. J. Med. Chem. 44, 619–626.

Sajan, D., Joseph, L., Vijayan, N., Karabacak, M., 2011. Natural bond orbital analysis, electronic structure, non-linear properties and vibrational spectral analysis of L-histidinium bromide monohydrate: a density functional theory. Spectrochim. Acta Part A: Mole. Biomole. Spectrosc. 81, 85–98.

Sharma, A., Suhas, R., Chandan, S., Gowda, D., 2013. Novel urea and thiourea derivatives of thiazole-glutamic acid conjugate as potential inhibitors of microbes and fungi. Russ. J. Bioorg. Chem. 39, 656–664.

Siddiqui, N., Arshad, M.F., Ahsan, W., Alam, M.S., 2009. Thiazoles: a valuable insight into the recent advances and biological activities. Int. J. Pharm. Sci. Drug Res. 1, 136–143.

Singh, G., Satija, P., Singh, B., Sinha, S., Sehgal, R., Sahoo, S.C., 2020. Design, crystal structures and sustainable synthesis of family of antipyrine derivatives: Abolish to bacterial and parasitic infection. J. Mole. Struct. 1199, 127010.

Siwek, A., Stączek, P., Stefańska, J., 2011. Synthesis and structure–activity relationship studies of 4-arylthiosemicarbazides as topoisomerase IV inhibitors with Gram-positive antibacterial activity. Search for molecular basis of antibacterial activity of thiosemicarbazides. Eur. J. Med. Chem. 46, 5717–5726.

Tota, J., Battu, S., 2018. Synthesis, Characterisation, biological activity and Docking studies of ternary metal complexes of Cu (II) and Co (II with 4-chloro-2-(2-Hydroxy) Naphthylidene Amino Benzothiazole Schiff base and Glycine ligands. Int. J. Pure Appl. Res. 1, 26–35.

Xavier, S., Periandy, S., Ramalingam, S., 2015. NBO, conformational, NLO, HOMO–LUMO, NMR and electronic spectral study on 1-phenyl-1-propanol by quantum computational methods. Spectroch. Acta Part A: Mole. Biomole. Spectrosc. 137, 306–320.